

resubmitted 1st November 2002

VLT/UVES Abundances in Four Nearby Dwarf Spheroidal Galaxies¹ II: Implications for Understanding Galaxy Evolution

Eline Tolstoy,

Kapteyn Institute, University of Groningen, PO Box 800, 9700AV Groningen, the Netherlands

Kim A. Venn,

Macalester College, Saint Paul, MN 55105, USA
University of Minnesota, 116 Church Street S.E., Minneapolis, MN 55455, USA

Matthew Shetrone,

University of Texas, McDonald Observatory, HC75 Box 1337-L, Fort Davis, Tx 79734 USA

Francesca Primas,

European Southern Observatory, Karl-Schwarzschild str. 2, D-85748 Garching bei München, Germany

Vanessa Hill,

Observatoire de Paris-Meudon, GEPI, 2 pl. Jules Janssen, 92195 Meudon Cedex, France

Andreas Kaufer & Thomas Szeifert

European Southern Observatory, Alonso de Cordova 3107, Santiago, Chile

¹Based on Ultraviolet-Visual Echelle Spectrograph observations collected at the European Southern Observatory, proposal numbers 66.B-0320, 65.N-0378, 62.N-0653 and 61.A-0275

ABSTRACT

We have used the Ultra-Violet Echelle Spectrograph (UVES) on Kueyen (UT2) of the VLT to take spectra of 15 individual red giant stars in the centers of four nearby dwarf spheroidal galaxies: Sculptor, Fornax, Carina and Leo I. We measure the abundance variations of numerous elements in these low mass stars with a range of ages (1–15 Gyr old). This means that we can effectively measure the chemical evolution of these galaxies *with time*.

Our results show a significant spread in metallicity with age, but an overall trend consistent with what might be expected from a closed (or perhaps leaky) box chemical evolution scenario over the last 10–15Gyr. We make comparisons between the properties of stars observed in dSph and in our Galaxy’s Disk and Halo, as well as Globular Cluster populations in our Galaxy and in the Large Magellanic Cloud. We also look for the signature of the earliest star formation in the Universe, which may have occurred in these small systems.

We notice that each of these galaxies show broadly similar abundance patterns for all elements measured. This suggests a fairly uniform progression of chemical evolution with time, despite quite a large range of star formation histories. It seems likely that these galaxies had similar initial conditions, and evolve in a similar manner with star formation occurring at a uniformly low rate, even if at different times. With our accurate measurements we find evidence for small variations in abundances which seem to be correlated to variations in star formation histories between different galaxies. The α -element abundances suggest that dSph chemical evolution has not been affected by very high mass stars ($> 15 - 20M_{\odot}$).

The abundance patterns we measure for stars in dwarf spheroidal galaxies are significantly different from those typically observed in the disk, bulge and inner-halo of our Galaxy. This means that, as far as we can tell from the (limited) data available to date it is impossible to construct a significant fraction of our disk, inner-halo or bulge from *stars* formed in dwarf spheroidal galaxies such as we see today which subsequently merged into our own. Any merger scenario involving dSph has to occur in the very early Universe whilst they are still gas rich, so the majority of mass transfer is gas, and few stars.

Subject headings: GALAXIES: ABUNDANCES GALAXIES: DWARF
GALAXIES: INDIVIDUAL (SCULPTOR, FORNAX, CARINA, LEO I)
STARS: ABUNDANCES

1. Introduction

With High Resolution Spectrographs on 8m class telescopes, such as UVES on VLT/UT2, we can take detailed spectra of individual stars in nearby dwarf galaxies and start to seek answers to detailed questions about the enrichment *history* of a variety of different elements within galaxies other than our own. It is critical to our understanding of galaxy evolution to accurately measure how the fraction of heavy elements in a galaxy builds up *over time*. It is impossible to accurately analyze a Color-Magnitude Diagram (CMD) and extract a unique star formation history (SFH) without some independent information on the metallicity of the stars and how this may have changed with time. The oldest stars we find in the nearby Universe are of an age similar to, if not greater than, the look-back time of the most distant galaxies found in the highest redshift galaxies known.

There are many theories as to how the chemical enrichment of subsequent generations of stars may occur in dwarf galaxies (*e.g.*, Silk, Wyse & Shields 1987; Pagel 1997), and there are also a significant number of measurements of nebular abundances and young stars today which undoubtedly carry the imprint of past enrichment patterns (*e.g.*, Matteucci & Tosi 1985; Pagel & Tautvaišienė 1998; Venn *et al.* 2001). However, extracting unique chemical evolution scenarios from these data is very difficult. The only way to accurately determine absolute abundances at different ages in the history of a galaxy is to take high resolution spectra of old low mass stars, with a range in age (color and luminosity). With extra-galactic stars in nearby galaxies we are forced to look at the brightest stars we can, which are Red Giant Branch (RGB) stars which were formed during the last 1–15 Gyr. The abundances of different elements provide an indication of the number and type of Supernovae enrichments which have proceeded the formation of these stars. Thus we can measure the evolution of these galaxies in great detail from the earliest times up to the epoch of last star formation. From previous studies there are well established techniques for detailed abundance analysis (*e.g.*, Shetrone, Bolte & Stetson 1998; Shetrone, Côté & Sargent 2001 [SCS01]; Hill *et al.* 2000 [H00]) which we can apply to the same type of stars in our sample of southern dwarf spheroidals.

Dwarf spheroidal galaxies (dSph) are intriguing systems. They are our nearest neighbors and so we can study them in great detail. Within the Local Group they are mostly satellites of larger galaxies such as our Galaxy and M 31 (*e.g.*, van den Berg 2000). Originally all dSph were believed to be essentially old systems similar to globular clusters, although there were hints to the contrary from the RR Lyrae stars and anomalous Cepheids which suggested that their underlying stellar populations were fundamentally different from those of globular clusters (*e.g.*, Baade 1963; Zinn 1980). Zinn suggested that the difference was due to the dSph systems being on *average* younger than globular clusters. Subsequent

deep photometric observations of the main-sequence turnoffs (MSTOs) in these galaxies confirmed the presence of intermediate age populations in some galaxies, and always an age spread at the earliest times, completely unlike most globular clusters. The dSph are typically small, faint and diffuse, non-nucleated systems, and yet they have complex SFHs. For most of these systems the SFHs have been accurately measured from main sequence turnoff photometry. These galaxies have typically no associated ISM, no HI gas (in the center), although there have been tentative detections of gas in the out lying regions of a few nearby dSph (*e.g.*, Carignan *et al.* 1998).

Despite considerable efforts with 4m class telescopes, many of the most basic questions remain unanswered for most of the Local Group dSph: How and when were they formed? Are they left over building blocks of our Galaxy? How has environment effected their evolution? To have a hope of addressing these complex and difficult questions we need to first answer such mundane ones as: What is the total range in $[Fe/H]$ for stars within a given dSph? Does the $[Fe/H]$ match that of our halo populations (Globular clusters or field stars)? Do the elemental ratios (particularly $[\alpha/Fe]$ and [r- and s- process/Fe] ratios) in dSph stars track those seen in the metal poor field or the globular clusters? In addition, there is strong evidence for a difference in the ratios of C, N, O, Na, Mg and Al to Fe between field population II giants and globular cluster giants (*e.g.*, Pilachowski *et al.* 1996; Shetrone 1996). This difference is presumably related to the extent to which deep dredging occurs in giants, but if (and how) this is ultimately caused by variations in environment between globular cluster and field stars remains a mystery. However, if the dSph are “globular-cluster-like” in this regard, it would present a problem for the idea that the Galactic halo is composed of dispersed dSph galaxies (*e.g.*, Zinn 1993; Shetrone 1998).

Detailed studies of the abundance patterns of stars in dSph can constrain the effects of discrete star formation episodes and different SFH on chemical evolution (*e.g.*, McWilliam 1997). UT2+UVES provides a unique opportunity (in the southern hemisphere) to extend detailed stellar abundance work to stars in external galaxies. This kind of study has only been possible so far with HIRES on Keck (*e.g.*, Shetrone, Bolte & Stetson 1998; SCS01), where it has been clearly shown that detailed abundance analysis of stars in nearby galaxies is feasible and can place important constraints on metallicity dispersions and what they mean for the metallicity evolution of nearby galaxies. We looked at samples of stars in four nearby dwarf spheroidal galaxies (dSphs): Sculptor, Fornax, Carina and Leo I. We also looked at four stars in three well studied stars in Galactic globular clusters (M30, M55, M68), to check that at least our calibrations put us on the same abundance scale as previous studies. Globular clusters also serve as an interesting comparison to the observations of stars in dSph.

In Sculptor and Fornax there are recently published low resolution Ca II triplet (CaT) spectra of a sample of RGB stars (Tolstoy et al. 2001; hereafter T01). These UVES data thus provide a detailed check of the CaT method which has been used to estimate iron abundances in RGB stars, based on calibrations in the Galaxy (*e.g.*, Armandroff & Da Costa 1991; Rutledge, Hesser & Stetson 1997).

From our high resolution spectra the most basic measurement that we can make is the iron abundance ($[\text{Fe}/\text{H}]$) in the atmospheres of these RGB stars. Iron is the typical element used to define the fundamental metallicity of a system. From high resolution spectra we typically have nearly 70 lines of Fe I and around 15 of Fe II which allows the determination of an exceptionally secure value for $[\text{Fe}/\text{H}]$ independent of the usual caveats and uncertainties accompanying the determination of abundance from a single line, and especially all the additional problems of measuring a different element (such as Ca or Mg) and converting this to $[\text{Fe}/\text{H}]$. From high resolution spectra there are also a host of other elements for which an accurate abundance can be obtained. These give us additional insights into the details of past star formation processes in these galaxies (cf. McWilliam 1997, and references therein).

Light Elements (*e.g.*, O, Na, Mg, Al) allow us to trace “deep-mixing” abundance patterns in RGB stars. This is a very distinctive pattern of abundances that are markedly different in globular cluster giants and field stars. There are also the group of α -elements (*e.g.*, O, Mg, Si, Ca, Ti), elements with even Z . The production of these elements is dominated by Type II Supernovae (SNII). They affect the age estimates based on RGB isochrones, as lower α -tracks are bluer than high α -tracks. The α -abundance limits the number of SNII explosions that can have polluted the gas from which the star was made, and thus contains estimates of the fraction of lost ejecta and/or IMF variations in the stellar populations of a galaxy through time. The Fe-Peak elements (*e.g.*, V, Cr, Mn, Co, Ni, Cu, Zn) are mostly believed to be the products of explosive nucleosynthesis. The level of the Fe-peak can (in principle) limit the most massive progenitor that can have exploded in the galaxy (*e.g.*, Woosley & Weaver 1995). Cu has been thought to be primarily produced in Type Ia Supernovae (SNIa), and hence $[\text{Cu}/\alpha]$ could be an indicator of the ratio SNIa/SNII. However, there is no physical basis for this assumption. It is also possible to account for Cu evolution in the halo using metallicity dependent SNII yields (*e.g.*, Timmes, Woosley & Weaver 1995). Heavy Metals ($Z > 30$, *e.g.*, Y, Ba, Ce, Sm, Eu) enable a distinction to be made between the fraction of s-process and r-process elements in a star, and thus again puts detailed constraints on the number and type of past SN explosions. The $[\text{Ba}/\text{Eu}]$ ratio can be considered an indicator of the contribution of AGB stars to the chemical evolution process. One has to be a bit careful since some stars can self pollute their $[\text{Ba}/\text{Eu}]$ ratio (but usually they stand out as having very large Ba/Fe ratios). Since AGB stars have a

several Gyr timescale for chemical contamination of the ISM they provide yet another type of clock.

By looking at dSph we are studying an environment which is metal poor ($[\text{Fe}/\text{H}] < -1.0$) and often with complex SFH. This describes the properties of the galaxies found to dominate deep redshift surveys and hence the Universe (*e.g.*, Madau, Pozzetti & Dickenson 1998). Indeed if the standard models of galaxy formation are to be believed, small dwarf galaxies are the oldest structures in the Universe (*e.g.*, White & Rees 1978; Moore *et al.* 1999; Klypin *et al.* 1999). Because dSph stars are relatively easy to age date from a CMD if (at least) $[\text{Fe}/\text{H}]$ is known (more accuracy is obtained if $[\alpha/\text{Fe}]$ is also known), and given that dSph *always* contain ancient stellar populations, there are potentially stars carrying the nucleosynthetic signature of the earliest epochs of star formation in the Universe (*e.g.*, Abel, Bryan & Norman 2002; Bromm, Coppi & Larson 2002; Heger & Woosley 2002). We make a comparison with the abundance patterns we observed in the oldest stars in the dSph with theoretical predictions of the formation of the first star(s).

2. Observations

We observed 15 individual RGB stars in 4 nearby southern dSph galaxies which we can add to the 17 RGB stars previously observed in 3 northern dSph with Keck/HIRES by SCS01 (see Table 1). We selected RGB stars to cover as much range in color as possible in each galaxy to sample the diversity in $[\text{Fe}/\text{H}]$ and age and thus gain an insight into how stellar abundances have varied over the history of the galaxies ($\sim 1\text{--}15$ Gyr).

Our observations were obtained in visitor-mode, with UT2/UVES (Dekker *et al.* 2000) on two separate visitor runs on Paranal, one in August 2000, and one in January 2001. We used the red arm of UVES, CD#3, centered at 580nm, which results in a wavelength range of 480-680nm. We obtained a resolution of $\sim 40\,000$ and average $S/N \sim 30$ per pixel. The integrations varied from 2–4 hours depending upon the brightness of the target and sky conditions. The details of the individual observations and the data reduction are contained in Shetrone *et al.* 2002 [hereafter, Paper I].

Covering the wavelength range 480-680 nm we detected a range of elements, including Fe I, Fe II, O I, Na I, Mg I, Ca I, Sc II, Ti I, Ti II, Cr I, Ni I, Y II, Ba II, Eu II, La II, Zn II, Cu I, Mn I (see Paper I for complete tables). This allowed us to achieve the comprehensive abundance analysis described in Paper I. We are able to make especially reliable abundance measurements because we determine abundances from *more than one line* for several elements, most crucially Fe II. The error analysis in abundance determinations from high

resolution spectra is complex and difficult, and the procedures and checks we carried out are described in detail in Paper I.

3. Results

3.1. Calibration Globular Clusters

We observed 4 previously studied stars in 3 globular clusters to verify our data reduction techniques and confirm that our abundances are consistent with previous measurements of the same stars with different instruments and telescopes (see Paper I). We have also compiled from the literature observations of other Galactic globular clusters (from SCS01), and also LMC star clusters (from H00; Hill & Spite 2001; Hill *et al.*, in prep) to compare the elemental abundance patterns typical in globular clusters with those found in dSphs.

The LMC clusters are in many ways the most reliable measures of abundance variations with time due to galaxy scale evolution because of the relative ease to age date globular cluster stars and the spread of ages in LMC clusters. The data set of H00 is a useful comparison with our results. Care should be taken in understanding the uncertainties in a few specific cases (see H00). Also direct comparisons between globular cluster and field star age-metallicity relationships are a little uncertain, because it is well known that the properties of star clusters do not always transfer readily to the field star population (e.g., Shetrone 1996). Nevertheless, the LMC star clusters provide an age-metallicity range with which to compare our results. Recent CaT measurements of a large sample of field stars in the LMC (Cole *et al.*, in prep) suggest that the LMC field star population follows the same age-metallicity relationship as the clusters (without the gaps).

3.2. The Dwarf Galaxies

For each of the four dSphs we used imaging taken at the NTT (Tolstoy *et al.* in prep), and supplemented by VLT archival images to select and determine the color of individual stars as targets for spectroscopic observation, and where possible we found radial velocity information about our targets from previous studies, which helps to a priori determine membership of stars in the dwarf galaxies.

From our UVES spectra we obtain an accurate [Fe/H] measurement for each star which allows us to compare its color and [Fe/H] with the appropriate isochrone set to determine

the age. The previous age determinations for the stars in Sculptor and Fornax from the CaT observations of T01 used Padua isochrones (Bertelli *et al.* 1994), which assume α -enhanced abundances ($[\alpha/Fe] = +0.5$), and as our high-resolution measurements suggest that in the mean dSph stars have roughly solar α -abundance we have redone the CaT age determinations using the new Yale-Yonsei isochrones (Yi *et al.* 2001), which assume solar α -abundance. This results in a small shift to older ages on average, but the trend (such as it is) doesn't seem to change markedly compared to T01. For our UVES spectra we have used exclusively the new Yale-Yonsei isochrones of Yi *et al.* to age date the stars observed (Table 2). Comparisons were made with Bergbusch & vandenBerg (2001) and Bertelli *et al.* (1994), see also Tolstoy (2002), and although there were differences no other set of tracks was significantly better (or worse) than another. We chose Yale-Yonsei because they went down to very young ages (unlike Bergbusch & vandenBerg) and they covered a range of α values down to zero. We also used the Yale-Yonsei isochrones to determine the ages of the dSph stars observed by SCS01 (see Table 3).

There is a marked degree of uncertainty in the ages determined from the RGB tracks, and an additional uncertainty coming from the errors on the measurement of $[Fe/H]$. There are some stars which do not fit *any* of the isochrones of the appropriate (observed) $[Fe/H]$ for a star. Typically they are too red (or too old) for any of the tracks, but sometimes too blue. This makes it clear that a simple global offset (*e.g.*, absolute photometric offset, reddening) doesn't solve the problem. It might be that there is more differential reddening in some of these galaxies than is realized. It is also possible that some of the stars which are on the blue side of RGB are in fact unidentified AGB stars (*e.g.* in Sculptor), and the stars on the red side of the isochrones are weak CH stars (*e.g.* Shetrone, Côté & Stetson 2001 found large numbers in Draco), which means their age cannot be determined from RGB isochrones. This might explain the large number of relatively young stars that we appear to identify in Sculptor from the CaT measurements. A basic look at the previous CMD analysis suggests that the majority of the star formation in this galaxy should have occurred more than 8–10 Gyr ago, and since the stars chosen here for metallicity measurements were randomly selected this ought to be reflected in the distribution of ages. Our sample of measured metallicities is still rather small. An example of the problems we have encountered in Sculptor and Fornax are plotted in Figure 1 and Figure 2. There weren't such severe problems in determining the ages of stars in the Carina and Leo I stars, as they fall into the expected color range of the appropriate theoretical stellar isochrones, but given the problems in Fornax and Sculptor all the isochrone ages should still be viewed with some caution.

We checked the Galactic Na I interstellar absorption line in all our spectra to try and understand how reliable the reddening estimates we have used might be. There is clearly

evidence for variation in line width between all the galaxies and also between individual stars in each galaxy. These variations could be interpreted as evidence for differential reddening, but the correlation between Na I line width and $E(B-V)$ is a very uncertain and complex problem (e.g., Munari & Zwitter 1997; Andrews, Meyer & Lauroesch 2001). The variations we find fall broadly into the scatter of this relationship.

Looking at where our spectroscopic targets lie in a CMD and comparing them to globular cluster RGB fiducials (Da Costa & Armandroff 1990) we found that globally speaking the more metal rich stars are to the red of the more metal poor, consistent with what you would expect from a population where the older stars have the lower metallicity. However, going from a determination of relative ages to absolute ages requires accurate isochrones. Our problems with isochrones suggest that perhaps there are more factors than age, $[Fe/H]$ and $[\alpha/Fe]$ that are required to uniquely define the correct isochrones for stars in dSph. This might be due to differences in stellar evolution in globular clusters from galaxies (e.g., different mixing lengths, rotation rates, binary fractions, etc), or perhaps more simply the theoretical stellar evolution models are not able to take into account the different abundance patterns in non-globular cluster stars (e.g., α -elements, and also the light elements). For example, Na is (along with K) by far the most important e^- donor in the atmosphere of an RGB star, and $[Na/Fe]$ is depleted in dSph stars relative to stars in most globular clusters. It seems that all isochrones have difficulty determining the ages of stars in galaxies, but this is not a problem in globular clusters (e.g., Tolstoy 2002).

There are main sequence turnoff star formation histories for all these galaxies, so we know which age range to expect, but it is clear that the only way to resolve these problems with isochrones in galaxies fully is to get more spectra and see if a pattern emerges. Not only in understanding the star formation processes at the formation epoch, but also in understanding the problems in matching low metallicity stellar evolution tracks to stars in these galaxies.

The previous CaT results from T01 are plotted in the following sections as small pink circles, and a representative error bar is also shown on the plot. No individual error bars are plotted for the CaT values, because they are too large, and make the plot unreadable (see T01). The new UVES results are plotted as symbols with individual error bars. The error bars are determined from the equivalent width measurement errors in the UVES spectra and the resulting uncertainty of this error on the age determination based on the range of isochrones within the $[Fe/H]$ error bars. We also plot for comparison other observations of age and $[Fe/H]$ for stars in the Galactic disc from E93 as small black dots, and the UVES study of the LMC clusters from H00 as light blue star symbols.

The dashed line(s) in the metallicity evolution figures describe the most simple

(closed-box) chemical evolution model (as first described by Searle & Sargent 1972). Searle & Sargent define a yield as the ratio of the rate at which an element is produced by nucleosynthesis and ejected into the ISM to the rate at which hydrogen is removed from the interstellar gas by star formation. We assume that these dSph galaxies have used up all their gas forming stars at the time of the last star formation in the galaxy. The $[\text{Fe}/\text{H}]$ they achieved in doing so is the metallicity of the most recent star formation. This allows us to determine the value of the yield as defined by Searle & Sargent for each galaxy, and assuming it is constant we can work back to how $[\text{Fe}/\text{H}]$ has varied over time by assuming that the star/gas ratio has been changing at the star formation rate determined from CMD analysis. This is ad hoc, but it provides a basic estimate of how $[\text{Fe}/\text{H}]$ may have varied as a result of the SFH of each dSph.

We also plot in each metallicity evolution figure as a dotted line the LMC age-metallicity relation as determined by the bursting model of Pagel & Tautvaišienė (1998).

The Galactic disk age-metallicity observations are included only as a broad based comparison, they have of course been differently determined coming as they do predominantly from spectra of main sequence turnoff stars. These have different errors and uncertainties from the RGB spectra we use. Reassuringly, abundance measurements of giants and subgiants in Galactic globular NGC 6397 (Castilho et al. 2000) find similar results to a study of main sequence turnoff stars in the same cluster (Thévenin *et al.* 2001). The Galactic disk abundances are a usefully large set of age-metallicity evolutionary measurements with which we can directly compare our evolutionary results.

3.3. Sculptor Dwarf Spheroidal

From the NTT CMD (Figure 3) we selected stars bright enough to be observed by UVES, and where possible we found radial velocity information about our targets from previous studies (Queloz, Dubath & Pasquini 1995; Schweitzer *et al.* 1995). The UVES targets, and the stars previously observed with FORS1 to measure the CaT metallicity are marked on Figure 3.

3.3.1. Star-Formation History

The first attempt to piece together an accurate star-formation history determined from a CMD reaching down to globular cluster age main sequence turnoffs was made by Da Costa (1984). He noted that the intrinsic width of the RGB was probably caused

by a 0.5 dex spread in abundance (from $[\text{Fe}/\text{H}] = -2.1$ to -1.6), and a population of “blue-stragglers” (in globular cluster terminology), which could be interpreted as main sequence turn-off stars as young as 5 Gyr old. Kaluzny *et al.* (1995) made a careful study of the central region of Sculptor and found no main sequence stars ($m_V < 21$), ruling out any star formation over the last 2 Gyrs. Using WFPC2, Monkiewicz *et al.* (1999) have made the deepest CMD of Sculptor to date, although they cover a tiny fraction of the entire galaxy. Their accurate photometry in this region allowed them to conclude that the mean age of Sculptor is similar to that of a globular cluster, but that there was probably a spread in age during this epoch of at least 4 Gyr.

Sculptor is known to contain a small number (8) of intermediate age carbon stars (*e.g.*, Frogel *et al.* 1982; Azzopardi *et al.* 1986), of which only 1 is a bona fide AGB star, the other 7 have been identified as CH stars (Martin Groenewegen, private communication). There is thus very little evidence for a significant metal poor intermediate age stellar populations (*e.g.*, Aaronson *et al.* 1984). Sculptor shows tantalizing evidence on its Horizontal Branch (HB) for an unusual enrichment history (Majewski *et al.* 1999; Hurley-Keller, Mateo & Grebel 1999).

Carignan *et al.* (1998) found evidence for small amounts HI gas in and around Sculptor, although this has recently been found to be part of a large scale complex, presumably Galactic HVC and unlikely to be associated to Sculptor (Lisa Young, private communication).

The SFH resulting from previous studies of the stellar population is plotted in Figure 4. Sculptor is the only predominantly old galaxy in our sample. It has thus much in common with the northern dwarf galaxy sample previously looked at with HIRES on Keck (SCS01).

3.3.2. *Metallicity Evolution*

From the CaT results of T01 it was suggested that the RGB stars across Sculptor contain a mean metallicity, $\langle [Fe/H] \rangle = -1.5$ with a significant spread $\delta[Fe/H] = 0.9$, larger than that predicted from photometry $\langle [Fe/H] \rangle = -1.8 \pm 0.3$ (Kaluzny *et al.* 1995; Da Costa 1984). The histogram plot shows a fairly sharp cut off in the upper $[\text{Fe}/\text{H}]$ boundary for Sculptor, with a shallow tail extending to low $[\text{Fe}/\text{H}]$. The highest metallicity observed was $[\text{Fe}/\text{H}] = -1.3$, and there are a few objects around $[\text{Fe}/\text{H}] = -2.1$, but the majority are clustered between $[\text{Fe}/\text{H}] = -2.0$ and -1.3 . There is no evidence for any spatial effect in the distribution of stars of different $[\text{Fe}/\text{H}]$. The dispersion is too large to be consistent with all the stars being similarly old. H400 is lying in a position in the CMD (see Figure 3) which might cause concern as to whether it is an RGB or an AGB star.

The CaT results, along with the new UVES results and the comparison observations described in §3.2 are plotted in Figure 5. There is broadly speaking an agreement between the UVES results and the CaT results. The observations suggest that Sculptor has had quite a similar metallicity evolution to that found for the old LMC star clusters of H00 in its earliest times, but not evolving so rapidly between 10 and 15 Gyr ago, consistent with very little star formation in Sculptor after this time. At 4–5 Gyr ago the star formation in Sculptor appears to have stopped altogether, and contrarily increased rapidly in the LMC and this is the period of largest deviation in the comparison between the two age-metallicity relationships.

The evolution of $[\text{Fe}/\text{H}]$ with age shown in Figure 5 is quite consistent with the closed-box chemical evolution scenario also plotted (and explained in §3.2). The largest uncertainties are the earliest enrichment at the epoch of the first star formation in this galaxy, where our data suggest quite a large spread in $[\text{Fe}/\text{H}]$.

3.4. Fornax Dwarf Spheroidal

From the NTT CMD (Figure 6) we selected stars bright enough to be observed by UVES, and we supplemented this list with targets from a previous spectroscopic study to determine radial velocities of stars in Fornax (Mateo *et al.* 1991). The UVES targets, and the stars previously observed with FORS1 to measure the CaT metallicity are marked on Figure 6.

3.4.1. Star-Formation History

Fornax is larger and more metal rich, in the mean, than the other galaxies in our sample. It also has (unusually for dSph galaxies, and uniquely in our sample) globular clusters. The extended sequence of main sequence turnoffs in the Fornax CMD indicates a long history of star formation (*e.g.*, Beauchamp *et al.* 1995; Stetson, Hesser & Smecker-Hane 1998; Buonanno *et al.* 1999), which has only recently ceased. The luminosity of the brightest blue stars show that Fornax cannot contain any stars younger than 100 Myr (Stetson *et al.* 1998). The numerous (~ 120) carbon stars with a significant age spread in the range 2-8 Gyr ago (*e.g.*, Azzopardi *et al.* 1999; Aaronson & Mould 1980, 1985) testify to extensive intermediate age star formation. This is supported by a well-populated intermediate-age subgiant branch and a red clump, which require a significant population with an age of 2-4 Gyr. Most recently, an HST study sampling the main-sequence turnoffs

of the intermediate-age and old populations in the center of Fornax was carried out by Buonanno *et al.* (1999), and they found evidence for a highly variable SFH starting at the epoch of globular cluster formation (~ 15 Gyr ago) and continuing until 0.5 Gyr ago. An ancient population is present as demonstrated by detection of a red Horizontal Branch, slightly fainter than the Red Clump (Buonanno *et al.* 1999), and of RR Lyrae variables (Stetson *et al.* 1998). There is also a weak, blue Horizontal Branch so Fornax clearly must contain only a small old, metal-poor component (despite having a globular cluster population).

Young (1999) looked for neutral hydrogen in and around Fornax and found none, to the column density limit of $4 \times 10^{18} \text{cm}^{-2}$ in the galaxy center, and 10^{19}cm^{-2} out to the tidal radius.

The SFH resulting from these previous studies of the stellar population is plotted in Figure 7. Fornax appears to have been forming stars until 2 Gyr ago, and to be dominated by an intermediate age (4–7 Gyr old) population, and has evidence for only a small number of globular cluster age stars in its field population.

3.4.2. *Metallicity Evolution*

From the CaT results of T01, the RGB stars selected across Fornax contain a mean metallicity, $\langle [Fe/H] \rangle = -1.0$ and a significant spread of $\delta[Fe/H] = 1.0$, which is slightly larger than that predicted from photometry $\langle [Fe/H] \rangle = -1.3 \pm 0.6$ (Beauchamp *et al.* 1995; Buonanno *et al.* 1985). In contrast to Sculptor, Fornax has more of a sharp cut-off in the $[Fe/H]$ distribution at low $[Fe/H]$, with a tail of values going out to higher values. This suggests different evolutionary influences. The highest $[Fe/H]$ observed is nearly solar and there are few objects at $[Fe/H] < -1.4$, with the majority clustered between $[Fe/H] = -0.9$ and -1.3 , with no evidence for any spatial effect in the distribution of stars of different $[Fe/H]$.

The CaT results, along with the new UVES results and the comparison observations described in §3.2 are plotted in Figure 8. There is broadly speaking an agreement between the UVES results and the CaT results. Fornax looks like it has had quite a similar metallicity evolution to that found for the LMC star clusters of H00. Of course with so few measurements, in both samples, it is difficult to say how close the similarities are. It looks like our CaT data at the oldest epochs contain a larger spread of $[Fe/H]$ than is seen in the LMC sample. Perhaps there should be more concern in the Fornax RGB for contamination by weak CH stars, given the large number of identified carbon stars in the galaxy. This might result in an over estimate of the ages of the oldest stars, and explain the rather high

[Fe/H] (apparently) observed in the oldest stars (in both CaT and UVES results). From the CMD analysis it is not expected that Fornax should have a very high star formation rate at oldest times, which makes it surprising that we apparently see quite a few old stars in the CaT sample. This is consistent with the hypothesis that we may have contamination of the RGB with weak CH stars.

The closed box chemical evolution model plotted on Figure 8 shows reasonable agreement with the [Fe/H] measurements going aback to about 10 Gyr ago. Before this period, during the epoch of earliest star formation in Fornax [Fe/H] is somewhat higher than might be expected. This could be due to the inherent uncertainty in determining the star formation rates at the oldest times. It resembles the G-dwarf problem know in our Galaxy (e.g., Pagel 1997) - there is an apparent lack of low [Fe/H] stars in Fornax, which is hard to explain within a simple enrichment model, starting from a zero metallicity proto-galaxy.

3.5. Carina Dwarf Spheroidal

From our NTT CMD we selected stars bright enough to be observed by UVES, and we supplemented this list with targets from a previous spectroscopic study to determine radial velocities of stars in Carina (Mateo *et al.* 1993). These stars had the advantage of known radial velocities. The UVES targets are marked on Figure 9 which is a VLT/FORS1 CMD made from archival data.

3.5.1. Star-Formation History

Carina was the first dSph galaxy to benefit from deep imaging in the early days of modern CCD detectors (Mould & Aaronson 1983) and remains one of the more spectacular examples of a dSph galaxy with significant variations in star formation rate with time, and a dominant intermediate-age population (Mighell 1990, 1997; Smecker-Hane *et al.* 1994; Hurley-Keller, Mateo, & Nemeč 1998; Hernandez *et al.* 2000; Dolphin 2002). The bulk of the stellar population in Carina has ages ranging from about 4 to 7 Gyr, though older (RR Lyr variables: Saha, Seitzer, & Monet 1986) and younger stars (or blue stragglers: Hurley-Keller *et al.*) are also clearly present.

The most recent quantitative star-formation histories for Carina (from two different data sets) are plotted in Figure 10. There are obvious differences between the three different SFHs. It is hard to normalise the absolute star formation rates between the three different

determinations, so this has been done in an arbitrary fashion. The main difference is that Hurley-Keller *et al.* (1998) in contrast to Hernandez *et al.* (2000) and Dolphin (2002) see discrete bursts of star formation. This might be because Hurley-Keller *et al.* are better able to resolve such details as they cover a much larger area of the galaxy and hence all the main sequence turnoffs are better populated than in the tiny HST field used by the other two studies. Also Dolphin and Hurley-Keller *et al.* find evidence of ancient star-formation (as expected from the RR Lyr population found by Saha *et al.* 1986), whereas Hernandez *et al.* do not. Another difference is the assumed $[\text{Fe}/\text{H}]$, not only the absolute value, but the spread. Dolphin finds $[\text{Fe}/\text{H}]=-1.2\pm 0.4$, where as Hurley-Keller *et al.* assumes $[\text{Fe}/\text{H}]=-2.1\pm 0.1$ and Hernandez *et al.* $[\text{Fe}/\text{H}]=-2.0\pm 0.2$. In comparison with our results here it looks like Dolphin is a little too metal rich, and the other two studies a little too metal poor. These different assumptions significantly affect the star formation history determinations, and particularly the age of the peak(s) in the star formation rate.

3.5.2. *Metallicity Evolution*

The photometry of Carina from wide field imaging reveals a very thin giant branch (*e.g.*, Hurley-Keller *et al.* 1998). Given the large age spread measured from Main sequence turnoff photometry in this galaxy, a metallicity spread has always been thought necessary to compensate and produce the observed narrow RGB. Our UVES results for 5 stars give an average abundance, $\langle [Fe/H] \rangle = -1.6$, with a spread $\delta[Fe/H] = 0.5$. This is different from previous determinations from CMDs, which gave $[\text{Fe}/\text{H}]=-2.0$, and a spread $\delta[Fe/H] < 0.1$ (Mould & Aaronson 1983; Smecker-Hane *et al.* 1994; Hurley-Keller *et al.* 1998). CaT spectroscopy of 15 giants in Carina (Da Costa 1994) resulted in a narrow average $[\text{Fe}/\text{H}]=-1.9 \pm 0.1$, with one giant more metal-poor ($[\text{Fe}/\text{H}] = -2.2$). This is significantly more metal poor than our UVES results, but similar to our results they found a very small spread in $[\text{Fe}/\text{H}]$.

We plotted the $[\text{Fe}/\text{H}]$ versus age measurements as blue star symbols in Figure 11. The several (different) SFHs (shown in Figure 10) are represented by a series of lines, all consistent with a very small spread in $[\text{Fe}/\text{H}]$. There is no resolvable difference between the three predictions. They are broadly speaking in agreement with the UVES results, with one outlier (M10) at lower $[\text{Fe}/\text{H}]$ than might be expected. This star is comparable to the previous CaT determinations, and may represent a small population at this metallicity (similar to the old LMC cluster metallicity) that we don't sample very well.

Carina is the faintest galaxy in our sample, although its mass and average $[\text{Fe}/\text{H}]$ are similar to Sculptor (see Table 1). There is only evidence for fairly mild evolution

(very small spread) in $[\text{Fe}/\text{H}]$, but the number of stars observed is still very small. Unlike Sculptor and Fornax, in Carina the metallicity evolution looks significantly different to the LMC measurements of H00. Carina has a metallicity evolution which is consistently lower than the LMC clusters. The one star (M10) which is more metal poor than might be expected from the amount of star formation creates a spread in $[\text{Fe}/\text{H}]$ at the oldest ages. The $[\text{Fe}/\text{H}]$ values from the independently determined SFHs suggest that the older stars in Carina should have $[\text{Fe}/\text{H}]$ similar to the older LMC clusters. However, our results suggest (as do those of Da Costa 1994) that at least a small fraction of stars in Carina are of very low $[\text{Fe}/\text{H}]$. This may represent the “shot-noise” in the self enrichment of this galaxy at the earliest epochs of star formation, or it might be a result of the highly variable SFH in Carina. The number of high resolution observations we have is still too small to quantify this accurately, but the hints are tantalizing (see also Paper I).

3.6. Leo I Dwarf Spheroidal

From the previous spectroscopic study of Leo I (Mateo *et al.* 1998) we selected stars bright enough to be observed by UVES. These stars had the advantage of known radial velocities. The UVES targets are marked on Figure 12 which is a VLT/FORS1 CMD made from archival data.

3.6.1. Star-Formation History

Leo I is the most distant galaxy in our sample and this along with the proximity on the sky of the bright Galactic star Regulus have made photometric studies difficult. The earliest observations of Leo I indicated a significant intermediate age stellar population: Hodge & Wright (1978) observed an unusually large number of anomalous Cepheids; carbon stars were found by Aaronson, Olszewski & Hodge (1983) and Azzopardi, Lequeux, & Westerlund (1985, 1986). High quality CMDs have recently revealed a horizontal branch well populated from blue to red in Leo I (Held *et al.* 2000), and subsequent observations were made of RR Lyr variable stars (Held *et al.* 2001) predicted from the detection of the Horizontal Branch population. Held *et al.* estimated a mean metallicity for Leo I RR Lyr stars of $[\text{Fe}/\text{H}]=-1.8$, using the relation derived by Sandage (1993) between the average period of the RRab variable stars in the Milky Way globular clusters and their metallicity. This might suggest that the oldest populations in Leo I (>10 Gyr) have a mean metallicity close to this value.

Sophisticated modeling of main sequence turnoffs in a deep HST CMD by Gallart *et al.* (1999) has given the most accurate information on the SFH of Leo I to date. The SFH they derived is plotted in Figure 13. Also plotted is a more recent determination by Dolphin (2002) based on the same data set. The Gallart *et al.* analysis suggests a smoothly varying metallicity evolution of the stellar population between $[\text{Fe}/\text{H}] = -1.4$ and $[\text{Fe}/\text{H}] = -2.3$ (consistent with the mean determined by Held *et al.*). Dolphin on the other hand found much higher metallicities, $[\text{Fe}/\text{H}]$ between -0.8 and -1.2 dex. This discrepancy shows the inherent uncertainties in determining $[\text{Fe}/\text{H}]$ from the color of the RGB for a galaxy with a significant intermediate or young stellar population. Surprisingly the SFHs look very similar from both studies. Similarly to the case of Carina our high resolution $[\text{Fe}/\text{H}]$ measurements seem to fall somewhat intermediate to the two photometric determinations.

3.6.2. Metallicity Evolution

The Leo I CMD reveals an RGB which, based on photometry, can (and has been) suggested to be either indicative of a broad range of metallicity in the galaxy ($[\text{Fe}/\text{H}] = -1.9 \pm 0.5$ dex; Gallart *et al.* 1999) or a narrower range of higher metallicity stars ($[\text{Fe}/\text{H}] = -1. \pm 0.2$ dex; Dolphin 2002). Our UVES results are only for 2 stars, which makes any statistical analysis difficult. The abundances are $[\text{Fe}/\text{H}] = -1.06 \pm 0.2$ and $[\text{Fe}/\text{H}] = -1.52 \pm 0.2$, which falls somewhat intermediate between the two CMD analyses, but with only two stars it is impossible to be conclusive. Clearly more spectroscopic data is needed for this to be confirmed.

We plotted the $[\text{Fe}/\text{H}]$ versus age measurements as blue stars in Figure 14. There is no resolvable difference between the two chemical evolution scenarios, and they both, broadly speaking, agree with the UVES results, although the (young) high $[\text{Fe}/\text{H}]$ point is slightly above what might be expected.

It is very difficult to say anything detailed about the metallicity evolution in Leo I with just two measurements. In comparison to the trend of the LMC star clusters from H00, there appears to have been no rise in enrichment levels at intermediate ages (~ 8 Gyr ago), consistent with a galaxy dominated by star formation occurring in the last 5 Gyr (Figure 13). The metallicity evolution in Leo I may be similar to that observed in Carina, with very little spread until quite recent times.

4. Other Elements

There is much more information in a high resolution spectrum than the iron abundance of a star. There are a host of lines from other elements which can be interpreted in terms of how the chemical state of the interstellar medium from which stars are made has varied over time. There are four broad categories into which elements are distributed depending upon their properties: Light Elements, α -Elements, Iron-Peak Elements and Heavy Elements. All provide pieces of the overall story of the chemical evolution history of the stellar populations in a galaxy.

Our sample of dSph galaxies has a very broad range of ages of stars, and this makes studies of the abundance variations with time possible. Most of the diverse (and complex) aspects involved in interpreting these kinds of measurements are covered Paper I. However here we would like to summarise those aspects we consider most crucial for gaining a clearer understanding of the global star formation properties of these galaxies and how they may have formed and evolved through time.

4.1. The α -Elements

The α -elements is a common collective term for some even-Z elements (e.g., O, Mg, Si, S, Ca and Ti), that are predominantly dispersed into the ISM in SNII explosions. They are typically over abundant in globular clusters and halo stars relative to (solar) disk stars. The traditional interpretation of the trend of $[\alpha/\text{Fe}]$ decreasing with time is that this is due to the time delay between SNII and SNIa (e.g., Tinsley 1979; Gilmore & Wyse 1991). In principle the mixture of different α -abundances can provide a clue as to the mixture of SN explosions that must have produced the enrichment seen in a star (e.g., Woosley & Weaver 1995), because different mass SN produce different proportions of α -elements.

We define an average α in the same way as SCS01, namely, as an average of Mg, Ca and Ti abundances ($[\alpha/\text{Fe}] = 1/3([\text{Mg}/\text{Fe}] + [\text{Ca}/\text{Fe}] + [\text{Ti}/\text{Fe}])$). There are different ways to define this since O, Mg, and Si dominate by mass and relative abundance they can also dominate the α -effects on chemical evolution models and isochrones. In Figure 15 we compare the distribution of α -elements in our data (the red and blue symbols as defined in the caption) and the Keck measurements made by SCS01 of northern dSph RGB stars (Draco, Ursa Minor and Sextans), as green triangles with similar measurements of disk stars (E93, black crosses); halo stars (McWilliam *et al.* 1995, open squares); Galactic globular cluster measurements (this work and SCS01, blue crosses); LMC star cluster measurements

(H00, blue stars). SCS01 did not work out ages for their dSph stars, and so we have made estimates based on the $[\text{Fe}/\text{H}]$ and color of the stars they observed (see Table 3).

We have plotted the α -abundances both in the “traditional” manner, against $[\text{Fe}/\text{H}]$ in the upper panel of Figure 15, and against age in the lower panel. Both provide differing insights as to how these galaxies may be evolving with time, and also how our observations compare with those of other galaxies. Plotting against age is more useful from the point of view of understanding chemical evolution, but it is not easy to find suitable measurements to compare our results with, as it is difficult to determine accurate ages for halo or bulge stars.

The dSph α -abundances when plotted against age in the lower panel of Figure 15 appear to follow the same distribution as those for the disk and the star clusters. However, if we look at the plot of $[\alpha/\text{Fe}]$ versus $[\text{Fe}/\text{H}]$ in the upper panel of Figure 15, the properties of dSph are clearly significantly different from the disk in the sense that although the levels and the variation with stellar age of $[\alpha/\text{Fe}]$ are similar between the disk and the dSph, this is all occurring at much lower $[\text{Fe}/\text{H}]$ in the dSph. The upper panel of Figure 15 also shows that the properties of the dSph differ from those typical of halo stars, although there is more overlap in $[\text{Fe}/\text{H}]$ values, the $[\alpha/\text{Fe}]$ of the halo stars are typically higher, although there is a population of low $[\alpha/\text{Fe}]$ halo stars which could conceivably be accreted satellite galaxies (e.g., Nissen & Schuster 1997). The star cluster measurements follow the upper envelope of dSph values, although most of the cluster stars show deep mixing abundance pattern. Thus the properties of $[\alpha/\text{Fe}]$ in dSph does not match globular clusters, nor the disk nor the majority of the halo.

4.1.1. *The Evolution of $[\alpha/\text{Fe}]$ due to star formation*

In Figure 16 we plot $[\alpha/\text{Fe}]$ for each dSph separately, over-plotted is an illustrative *estimate* of the variation of $[\alpha/\text{Fe}]$ for each galaxy *given the star formation rate variation*. There really are not sufficient data on these galaxies to be certain that we are seeing direct evidence of evolution in $[\alpha/\text{Fe}]$, but the results are highly suggestive. The dashed lines are not derived from the SFH directly, but a knowledge of the SFH is used to find the most likely pattern with time in the α -abundances. Carina has the most impressive evidence for evolution of abundances due to variations in star formation rates with time. The variations seen in $[\alpha/\text{Fe}]$ are supported by consistent variations in Ba, La, Nd and Eu (see Paper I). With the exception of Carina, the star formation histories *inferred* from $[\alpha/\text{Fe}]$ are consistent with the CMD SFH described in §3. In Carina it is possible that due to the incorrect metallicity evolution assumed in all the CMD SFH determinations described in

§3.5.1 that the SFH has not been well determined. Figure 16 suggests that there has been an ancient epoch of star formation (13–15 Gyr ago), followed by a hiatus, then another epoch of star formation 9–11 Gyr ago. More data are clearly required to quantify this interpretation of these data.

One curious point is that in all our observations $[\alpha/\text{Fe}]$ is roughly solar for the oldest stars. This might be a remnant of the initial enrichment of the dSph gas in the early universe, by a process which is quite different from the star formation processes that we see today. This is certainly not consistent with what would be expected for stars switching on in a zero (or close) metallicity environment. It ought to take time for the $[\alpha/\text{Fe}]$ to get to zero (e.g., Pagel & Tautvaišienė 1998).

4.1.2. Comparison with Common “Metallicity” Determinants

In Figure 17 we plot three elements of particular interest against age, using the same symbol definitions in Figure 15. We choose to look at $[\text{O}/\text{Fe}]$ against age in the upper panel because O is so abundant, and thus arguably the best “metallicity” tracer. In middle panel of Figure 17 we look at $[\text{Ca}/\text{Fe}]$ because of our interest in accurately interpreting CaT results, The high resolution measurement of the $[\text{Ca}/\text{Fe}]$ abundance is a useful test of the reliability of the conversion between CaT observations and $[\text{Fe}/\text{H}]$. Another common tracer of $[\text{Fe}/\text{H}]$ from low resolution spectra is $[\text{Mg}/\text{Fe}]$ which we plot in the lower panel of Figure 17. We also plot in all the panels of Figure 17 the E93 disk abundances as black crosses.

There is quite a large scatter in the $[\text{O}/\text{Fe}]$, especially at the earliest times. It follows the same trend as the disk abundances, but the scatter is somewhat larger than seen in the disk at earlier times, often similar to the halo enhancement. The relatively young (~ 2 Gyr old) LMC star cluster NGC 1978 appears to have a very high oxygen abundance, but this is a very insecure measurement (see H00).

The $[\text{Mg}/\text{Fe}]$ results look very similar to the $[\text{Ca}/\text{Fe}]$, with slightly greater spread in the $[\text{Mg}/\text{Fe}]$ values. These values are also fairly similar to the results from the disk stars. They are very close to solar with little or no discernible trend, although in common with $[\text{O}/\text{Fe}]$ the dSph measurements appear to have a larger scatter at the oldest ages than is seen in our disk. Looking at the 3 stars we observed in Fornax, they appear to have a fairly constant above solar value Ca abundance ($[\text{Ca}/\text{Fe}] \sim 0.25$), and no similar enhancement in $[\text{O}/\text{Fe}]$ or $[\text{Mg}/\text{Fe}]$. There have been breaks in the α -abundance patterns seen before (e.g., in the bulge, McWilliam & Rich 1994), but these previously observed patterns are different to those we observe in Fornax. The reasons for these breaks are not clear. Obviously

considerable care has to be exercised in interpreting metallicity determinations based on CaT and Mgb lines. They are clearly statistical measurements requiring large samples of stars.

4.1.3. Interpretation of $[\alpha/\text{Fe}]$ observations

The low $[\alpha/\text{Fe}]$ values found in the disk stars of our Galaxy have been interpreted as evidence for star-formation in material with a large fraction of SNIa ejecta. This is perhaps not surprising for our disk, with high metallicity, and typical predictions of fairly recent formation (from enriched material). It is not clear that the same assessment can be made of the similarly low $[\alpha/\text{Fe}]$ in dSph galaxies. Everything we know about dwarf galaxies suggests that they have never had very high rates of star formation. The stars in dSph typically have much lower $[\text{Fe}/\text{H}]$ and $[\text{O}/\text{H}]$ than in our disk. A low star formation rate may explain the low $[\alpha/\text{Fe}]$ values because the SNII products may predominately come from low mass SNII ($8\text{--}12M_{\odot}$ progenitors), which result in lower α yields than their higher mass cousins (*e.g.*, Woosley & Weaver 1995). This is (unfortunately) effectively a truncated IMF, but it is motivated by the likelihood that in the physical conditions to be found in small galaxies the probability of forming high mass molecular clouds (and thus high mass stars) is low. The variations in $[\alpha/\text{Fe}]$ shown in Figure 16 are suggestive that $[\alpha/\text{Fe}]$ does vary with star formation rate, but more data are needed to confirm and quantify this.

4.2. Iron-Peak Elements

The Iron-peak elements (*e.g.*, Cr, Mn, Co, Ni, Cu, Zn) are the highly stable end-products of the nucleosynthesis sequence by nuclear fusion, and they provide the seeds which capture neutrons and produce heavy elements. It is hard to find suitable comparison samples with known ages for heavy element abundances because it seems that none of the observations of these elements have been made of stars of known age. Generally speaking it seems that dSph stars have halo-like Iron-Peak abundance patterns (see Paper 1). Two important Fe-peak elements with regard to understanding galaxy evolution and also making the connection between galaxies observed in the nearby and more distant Universe are Zn and Cu.

4.2.1. Zinc

Zn plays a pivotal role in interpreting the abundance patterns of the Damped Lyman Alpha systems (DLAs), so it is interesting to compare it with the values measured in the nearby universe. In Figure 18 $[\text{Zn}/\text{Fe}]$ is plotted versus $[\text{Fe}/\text{H}]$. The dSph observations are plotted using the same symbols defined in Figure 15. Also plotted in Figure 18, for comparison, compilations of $[\text{Zn}/\text{Fe}]$ for disk and halo stars obtained from the literature (*e.g.*, Sneden, Gratton & Crocker 1991), plotted as black stars, and the black open circles are a selection from the new sample of disk and halo star measurements from Primas *et al.* (2000). Also plotted are the values measured in D $\text{Ly}\alpha$ absorption systems at cosmological distances by Pettini *et al.* (2000), as black circles, with purple error bars. The DLA $[\text{Zn}/\text{Fe}]$ measurements at high redshift are, on average, higher than anything else observed in the Local Group (see Figure 18). This is largely due to depletion of Fe onto dust grains. In fact, these particular DLAs were selected by Pettini *et al.* as those that showed the lowest dust depletions such that the gas phase Zn results should represent the total Zn abundance quite well. The fact that they are quite homogeneous could imply that the Zn abundances are quite uniform in these DLA systems, but of course the uncertainties in the dust corrections complicates the interpretation. Also, the DLA measurements are very different from all others in Figure 18, coming from absorption of quasar light in the interstellar gas of an intervening galaxy.

The nucleosynthetic origin and history of Zn is not well understood (see Paper 1). Traditionally, Zn has been thought to be produced by s-process neutron capture reactions, but then it should decrease with metallicity (*e.g.*, Matteucci *et al.* 1993). Another possible site of Zn production is explosive Si-burning in SNII. Recent computations (Umeda & Nomoto 2002) suggest that the over-solar $[\text{Zn}/\text{Fe}]$ values found in the most metal-poor stars of our Galaxy are the result of deep mixing of complete Si-burning material and significant fall-back in SNII. It is clear that Zn is a key element to further constrain the physics of SNII explosions, but more data will be needed (also of other elements) before being able to discern among the different possible solutions (*e.g.*, Primas *et al.* in prep., from the VLT Key Programme 165.N-0276).

4.2.2. Copper

In the case of Cu, it has been suggested that the most significant production occurs in SNIa (*e.g.*, Matteucci *et al.* 1993). Cu is clearly underabundant with respect to Fe in all our observations of dSph (*e.g.*, Figure 19). They resemble the halo star Fe-peak abundance

patterns, which might suggest a lack of SNIa enrichment of the dSph ISM, but given that dSphs also show lower α -abundances relative to metal-poor halo stars (Figure 15) interpreted as a low SNII rate (relative to SNIa), it is not clear that this simple explanation is valid here. In Paper I we suggest that Cu is not produced readily in *low metallicity* SNIa. Another possible explanation is that dSph galaxies rarely form very massive stars (i.e. $> 15M_{\odot}$, see §4.1). SNII explosions at the low mass end of the possible mass range agree with the solar $[\alpha/\text{Fe}]$ measurements and also with the apparent underproduction of heavy elements. It is also possible to invoke metal dependent SN yields (e.g., Timmes *et al.* 1995; see discussion in Paper I).

$[\text{Cu}/\alpha]$ has been supposed to be a good indicator of the ratio of SNIa/SNII, assuming that Cu is predominantly made in SNIa, and α -elements are predominantly SNII products. Our data do not support this though. $[\text{Cu}/\alpha]$ is very low (halo-like) in all of the dSph stars (with the exception of the most metal rich star in Fornax; see Figure 19). Also, $[\text{Cu}/\alpha]$ is remarkably constant with age. This again suggests that Cu is not significantly produced in the *low metallicity* SNIa, like alpha-elements, especially given the star formation histories in these galaxies and the expected SN Ia contributions before <5 Gyr when the Cu abundance begins to increase.

4.3. The Heavy Elements

The Heavy elements are defined as those elements beyond the iron peak ($Z>31$). Heavy elements can only be synthesized by repeated neutron captures onto to Iron-peak elements followed by β decay. This can happen either slowly, with respect to the time for β decay (s-process) or rapidly (r-process), and these two processes are the result of different neutron sources and lead to different abundance patterns.

Ba is thought to be a predominantly s-process element, which is thought to mainly occur in low mass ($1 - 3M_{\odot}$) AGB stars (e.g., Truran 1981; Busso *et al.* 1995; Lambert *et al.* 1995). Eu is a nearly pure r-process element and thought to be produced only in SNII. It is typically enhanced in the stars measured in dSph, as is in our halo. This is also true for all but the oldest of the LMC star clusters. This is perhaps somewhat at odds with the relatively low α -abundances measures in the dSph stars, but consistent with our interpretation of α -element and Fe-peak abundances being predominantly from low mass SNII (predominantly $8-12 M_{\odot}$) in dSph, as discussed in §4.1 and §4.2.

In Figure 20, we have plotted the $[\text{Ba}/\text{Eu}]$ abundances, the symbols and the comparison data is the same as in Figure 15 in §4.1. As in previous figures we plotted the same data twice, once in the more traditional manner against $[\text{Fe}/\text{H}]$, in the upper panel of Figure 20,

and again versus age to put the data directly in an evolutionary context, in the lower panel. Examination of these two figures gives us an idea of the mix of s and r-process products in the stars in our sample, which allows us to assess the contribution of AGB stars to the chemical evolution of dSph as compared to low mass SNII. In the lower panel of Figure 20 we can see that, with the exception of one star (in Ursa Minor, which is clearly s-process contaminated, with a huge over abundances of the s-process elements compared to Eu), that the older stars in our sample show *predominantly* r-process heavy elements. This is similar to the older disk stars, and appears to evolve with time to include more and more s-process heavy elements. In the upper panel of Figure 20 we can see that the same domination of r-process elements is present in the halo and bulge stars, although there is some scatter. The LMC star cluster results plotted in the upper panel of Figure 20 show either a balance of r- and s-process elements, or perhaps a slight enhancement of s-process elements. This is different from the Galactic globular clusters and the halo stars (in the mean), and more similar to the younger disk stars (see also the lower panel of Figure 20).

The heavy elements in the oldest stars in the Universe must come from the r-process, because AGB stars have not yet had time to evolve and contribute to the ISM (takes at least ~ 1 Gyr). In both panels of Figure 20 we see a trend of increasing contribution of s-process elements with increasing $[\text{Fe}/\text{H}]$ (and age) across the disk, halo and also the dSph sample, consistent with the interpretation that it takes a few Gyr for the low mass stars created in the earliest star formation epochs to start producing enough s-process elements to influence subsequent generations of stars. Our data allows us to constrain this delay in our sample of dSph galaxies until about ~ 10 Gyr ago. It is at this time that s-process contributions start to match those of r-process elements, at least in Fornax, Sculptor and Carina. It doesn't look like Leo I ever reached this stage, nor Draco. But as in all our conclusions, this is uncertain due to the small number statistics here.

5. Implications for Understanding Galaxy Evolution

Having such detailed information, albeit on very few stars, it is interesting to try and put our results into a context that can be understood in terms of the implications for our understanding of galaxy evolution. This has been termed *Chemical Tagging* by Freeman & Bland-Hawthorn (2002), and is probably the only way to accurately disentangle the different phases in a galaxy's evolution back to the epoch of formation, tagged by the ever increasing enrichment of an interstellar medium by elements produced in stars and liberated in supernovae explosions or stellar winds. The galaxies we are concentrating on, dSph, are arguably very simple objects with regard to chemical evolution. They are like a single cell star forming entity. They are small potentials in orbit around a much larger one

and are thus unlikely to accrete much (if any) extraneous matter during its lifetime (either intergalactic gas, or galaxies) because they will typically lose the competition with our Galaxy. Their evolution is going to be influenced, maybe strongly, by the presence of our Galaxy. They will permanently lose gas to our Galaxy if it is expelled too far from their centers, and the dynamical friction of the orbit may have a strong influence on the rate of star formation at any given time in these galaxies.

5.1. Similar Abundance Patterns: Consistent Star Formation Mode

One aspect of these dSph RGB abundances which clearly stands out is how uniform they appear to be in general, despite a range of different star formation histories, and also how different they are from the properties of stars observed in the disk and halo of our Galaxy (*e.g.*, α -abundances, Figure 15). It is as if all stars know the mass of the potential in which they are forming.

Figure 16 suggests that with our UVES results we can trace the variation of $[\alpha/\text{Fe}]$ with time caused by varying (but always low) star formation rates at different times. This is the first time it has been possible to directly *measure* the $[\alpha/\text{Fe}]$ evolution of a stellar population over Gyr time scales, back from the earliest epoch of formation to the most recent star formation. The range of variation of alpha is quite small (which means accurate measurements are required to observe it), and it never reaches the parameter space where the disk and halo are stars predominantly to be found. So probably star formation, when it occurs, always occurs at similarly low levels in these small galaxies. Perhaps this is not surprising as it is the mass of cool HI gas in conjunction with the ability of the gravitational potential to compress it that determines the size and number of molecular cloud complexes which can form stars in a galaxy. It seems very unlikely that dwarf galaxies have ever experienced a very high star formation rate, and have thus had very few (if any) SNII of masses more than $15 - 20M_{\odot}$.

Thus it seems as if the *classical* interpretation of $[\alpha/\text{Fe}]$ as applied to the disk and halo of our Galaxy doesn't work when applied to dSph. It is possible to produce solar $[\alpha/\text{Fe}]$ values from very low star formation rates. Assuming a Salpeter IMF and using the predicted yields from Woosley & Weaver (1995), an event which forms $2500M_{\odot}$ of stars (over 10^7 yrs; $\text{sfr} \sim 2.5 \times 10^{-4} M_{\odot} / \text{yr}$) reduces O and Mg by a small amount ($\sim 0.1 - 0.15$ dex) and has no net effect on Si. However, for an event which forms only $1000M_{\odot}$ stars ($\text{sfr} \sim 10^{-4} M_{\odot} / \text{yr}$) the affect on O, Mg and Si is significant ($\sim 0.5 - 0.6$ dex). This means that a low star formation rate can explain the low $[\alpha/\text{Fe}]$ we observe in these galaxies. It also means that $[\alpha/\text{Fe}]$ will not be a good indicator of SNIa rates in systems with few

massive SNII.

5.2. Chemical Evolution: Evidence for infall or outflow

It is somewhat uncertain if these systems were (or are) small enough to lose significant mass (and metals) in SN explosions. This is partly due to problems determining the total mass of these small galaxies, both today and ascertaining what they may have been in the past. If we believe current estimates (*e.g.*, Mateo 1998, and references therein), these galaxies are currently of low enough mass that they are easily in the mass-range where supernova explosions ought to result in a significant metal-enriched blow-away, (*e.g.*, Mac Low & Ferrara 1999; Ferrara & Tolstoy 2000; Mori, Ferrara & Madau 2002). Blow-away means that it is unlikely that these galaxies would easily lose their entire interstellar medium in this fashion, but they may suffer metal enriched winds, where the metals may leave the system but the gas probably will not. Even if the metal enriched winds escape the central regions of the galaxy, it seems likely that they will continue to exist in a bubble surrounding the galaxy (*e.g.*, Ferrara, Pettini & Shchekinov 2000; Mori, Ferrara & Madau 2002), and therefore may still play a role in future star formation episodes. If dwarfs have a more extended DM halo than currently thought (*e.g.*, Kleya *et al.* 2002) these metal rich bubbles will be smaller, and more likely to collapse back into the central potential. None of the dSph around our Galaxy contain evidence for any particularly violent or intense star formation episodes in their past, so the typically high (simultaneous) SN rates assumed in simulations modeling the blowout properties are unlikely to occur in dSph, *e.g.*, Mori *et al.* assume a $\text{sfr} = 0.03M_{\odot} / \text{yr}$, which is much higher than is thought to be typical for small dwarfs ($\sim 10^{-4}M_{\odot} / \text{yr}$). However it is difficult to distinguish between low yields due to a low star formation rate and low yields due to mass loss. Another possible explanation is that the products of more massive ($> 20M_{\odot}$) SNII are predominantly lost to these galaxies, but it is hard to find any plausible reason why this might be so.

With the exception of the earliest times all abundance properties in these dSph are consistent with closed-box evolution as inferred from the star formation histories (Figures 5, 8, 11 & 14). Our data are not sufficient to rule out a leaky box scenario where some (small) fraction of the metals are lost. The implication is that outflows (and inflows) of metals are not necessary to explain the chemical evolution observed through most of the history of any of these systems. Gas and metals may flow out from the galaxy (*e.g.*, Mac Low & Ferrara 1999; Mori, Ferrara & Madau 2002) but, with the possible exception of the initial burst of star formation, there is a chance that they will return on a timescale ($< 1 - 2\text{Gyr}$) compatible with the evolutionary timescale of star formation in these galaxies.

It is possible that the large scale differences we see in star formation histories of dSph result from their differing orbits around our Galaxy (*e.g.*, Oh, Lin & Aarseth 1995). Tidal perturbations can significantly effect star formation, either compressing the ISM and increasing the star formation rate, or inhibiting it by stretching the galaxy, or even stripping the ISM altogether and thus stopping star formation for good, independent of the star formation rate in the galaxy. Some galaxies apparently lost (or used up) all of their gas very quickly (in a few Gyr), and others have managed to continue forming stars until very recently, but all seem to maintain similar chemical abundance patterns across time, until perhaps the last few Gyr. This suggests that the properties of star formation have not changed significantly over time. There is evidence for slow evolution in both the SNIa/SNII ratio, and the increasing contribution of s-process elements over time. There is no significant evidence for large discrepancies in abundances such as might be expected from gas renewal at some point in the life of a galaxy from a pristine source, but more data are required to make more firm conclusions.

5.3. Building Large Galaxies from Smaller Ones

One of the fundamental pillars of CDM theory is that small galaxies are the building blocks of larger ones (*e.g.*, Navarro, Frenk & White 1995). The timescale on which this build up of material occurs has been a matter of some discussion between the classical approach to modeling within the CDM paradigm which results in the prediction that galactic disks and halos (such as our own) have relatively recently experienced significant accretions of smaller galaxies (*e.g.*, Steinmetz & Navarro 2002; Kauffmann, White & Guiderdoni 1993), and those approaches which, independent of assumptions from CDM, utilise observations of our Galaxy and the nearby Universe to place limits on the star formation rates for all the different components in our Galaxy over a Hubble time (*e.g.*, Prantzos & Silk 1998; Rocha-Pinto *et al.* 2000).

Our results unequivocally show that the stars observed in dSph galaxies *today* (many of which are extremely old) *cannot* be used to make up the majority of stellar mass in our Galaxy, neither in the disk nor in the inner-halo (nor the bulge) because their nucleosynthetic signatures are not compatible. This places a limit to the age at which the majority of merging of small halos can have occurred, if it is to have occurred. This is of course assuming that these small halos are similar to the dwarf galaxies we see today. The majority of these kinds of mergers must have occurred very early, in the first few Gyr of structure formation, because this is the only way to ensure that the large potentials accrued mostly gas and very few stars, and so the majority of star formation will occur in a much larger potential than a dwarf galaxy with a lot more influence from massive SNII which is

required to explain the abundance patterns seen in our Galaxy, but not found in dSph. In this scenario there still remains the mismatch in the M/L between dwarf and giant galaxies; dwarf galaxies are frequently dark matter dominated, unlike large spiral galaxies.

Of course our dSph results do not place any limits on the effect of significantly larger accretions, (*e.g.*, LMC like objects). The detailed abundance measurements of old and intermediate age stars in the Magellanic Clouds are rather sparse, and so the conclusions are inherently uncertain, but there are suggestions that the abundance patterns of the stellar population observed in the Clouds and nearby dwarf irregulars do not resemble our Galaxy anymore than the dSph do (*e.g.*, Hill 1997; H00; Venn *et al.* 2002, in prep).

The only component of our Galaxy which could plausibly contain a significant contribution from stars formed in accreted dwarf galaxies is the halo, and it contains only about 1% of the stellar mass of our Galaxy (*e.g.*, Morrison 1993), and only a fraction of this, the outer-halo ($\sim 10\%$), could plausibly include stars accreted from dwarf galaxies (*e.g.*, Unavane, Wyse & Gilmore 1996). The outer-halo stars typically have different properties from the inner-halo which include relatively lower α -abundances, more consistent with those observed in dwarf galaxies (Nissen & Schuster 1997). However, the kinematic properties of these stars are not always consistent with what we see in satellite galaxies today (*e.g.*, Gilmore & Wyse 1998). The samples of well studied halo stars are still too small to be reliably quantitative or conclusive on any of these issues.

5.4. Did the “First Stars” form in dSph?

In CDM cosmology dwarf galaxy sized objects are the first structures to collapse in the early Universe. These first objects, arguably proto-galaxies, are predicted to have a total mass (dark + baryonic matter) of $\sim 10^6 M_\odot$ (White & Rees 1978; Tegmark *et al.* 1997). Within the CDM paradigm most of these small structures will merge to form much larger galaxies, such as our own, but a fraction may be supposed to survive until today in something like their original form. Within these first objects the first generation of stars in the Universe may form (zero metallicity), perhaps as one massive star (Abel, Bryan & Norman 2002; Bromm, Coppi & Larson 2002). So far it has been difficult to constrain the final mass of the “first” stars. Current predictions place them between 30 and $300 M_\odot$. Such a large uncertainty makes reliable nucleosynthetic predictions difficult.

These first collapsed proto-galaxies at $10^6 M_\odot$ have a mass which in most models is very close to the limit where star formation results in significant blow-out and disruption of the ISM and the total blow-away of all the gas in the galaxy in a SN explosion (*e.g.*, Larson 1974; Dekel & Silk 1986; Mac Low & Ferrara 1999; Ferrara & Tolstoy 2000; Mori,

Ferrara & Madau 2002). Thus, the formation (and subsequent SN explosion) of high mass stars (of order $100M_{\odot}$) in such small halos in the early Universe has also been recently invoked as a convenient way to pollute the early Universe with metals (*e.g.*, Madau, Ferrara & Rees 2001), and explain the relatively high abundance of metals in the IGM at quite high redshift, remove the G-dwarf problem in our Galaxy, and even to reionise the Universe (*e.g.*, Oh *et al.* 2001).

As a means of testing the idea that very massive stellar objects (VMOs) may have exploded at early times in small dwarf galaxy like objects which have survived until the present day as dSph, we look for their nucleosynthetic signature in the spectra of the oldest stars our sample, as predicted by Heger & Woosley (2002). We are not looking directly for Population III objects, but we are looking for any sign that the stars we observe were polluted by VMOs in the early Universe. In Figure 21 we plot the comparison of the abundances we observe in the only predominantly old galaxy in our sample, the Sculptor dSph with the predictions of Heger & Woosley for the SN products of a zero metallicity VMO. We also plot as a comparison the average abundance pattern seen in the most metal poor halo stars (in the range $-3 < [\text{Fe}/\text{H}] < -4$, from McWilliam *et al.* 1995).

The Sculptor dSph abundance patterns are very halo-like despite having significantly higher $[\text{Fe}/\text{H}]$ and lower average $[\alpha/\text{Fe}]$ not obvious in this plot, where all abundances are relative to α -element, Mg. Comparing the Sculptor abundance patterns with those predicted by the VMO pair-production SN (progenitor masses between $140M_{\odot}$ and $260M_{\odot}$) models of Heger & Woosley we can't find a good match. It is likely that all the stars in our sample have been enriched by more than one SN, although perhaps not many more (see Paper I). Most critically we always find elements heavier than Zn in all our spectra, which are absent in the Heger & Woosley VMO pair-production SN. This does place limits on the models which anticipate only one zero metallicity SN per proto-galaxy, but a lot more data are required to be conclusive.

The initial enrichment of the ISM in these galaxies is likely to develop extremely quickly as a result of the first star(s) formation. The time scale for SNII, is of order $< 10^6$ yrs, so the initial enrichment time scale of the ISM is well beyond the time resolution of our CMD analysis. Since we are only looking at 2–5 stars per galaxy we are not very likely to find a sample which represents the earliest most rapid phases of ISM enrichment. We need to observe abundances for a much larger sample of stars in these dSph to build up an accurate picture of how the early enrichment may have progressed on the very short timescales of the initial enrichment. It is possible, at least for dSph, that varying rates of loss of gas and metals in SN driven winds in the earliest starburst phase of formation make our understanding of the abundance patterns in the oldest stars very complex.

6. Conclusions

We have obtained high resolution VLT UVES spectra for 15 RGB stars in Sculptor, Fornax, Carina and Leo I dSph galaxies. Adding this to the previous Keck HIRES observations of 17 RGB stars in Draco, Ursa Minor and Sextans dSph by SCS01 we have a sizable sample of stars with which to study the chemical evolution of our smallest neighbors. We have measured abundances for more than twenty different elements in all these stars, and used these many different indicators to try and constrain our understanding of chemical evolution in dwarf galaxies back to the earliest times.

Our results, similar to SCS01, show a very uniform abundance pattern across all these galaxies. This is evidence for very similar chemical evolution histories in all dSph galaxies, similar initial conditions and a similar IMF. It was initially a surprise that the abundance patterns were so similar since these galaxies have often quite different star formation histories, and all of the galaxies have evidence for fairly large spreads in $[\text{Fe}/\text{H}]$ (see Table 5). The fact that these galaxies have always had very small (but variable) rates of star formation is consistent the patterns we see in the α -, Fe-Peak and Heavy Element abundances. These variations are fairly well behaved. We also find that the global increase in $[\text{Fe}/\text{H}]$ with time does not require (or indicate) any significant infall or outflow of gas or metals from these systems, but this is very dependent on the accuracy of the models used to determine yields.

A small star formation rate could also have the effect of limiting the impact of massive SNII on the chemical evolution of these galaxies, effectively truncating the IMF, which could account for the marked difference between the abundance patterns seen in dSph stars and those found in our Galaxy. This data set allows us to infer more clearly the effects of AGB star mass loss and low mass SNII on the chemical evolution of a galaxy. In our Galaxy detailed signatures of this kind of enrichment may often be “washed out” over time, possibly because the chemical properties of a system which has high mass SNII will (not surprisingly) be totally dominated by them. It might also be possible to explain the abundance patterns in terms of mass (and metal) loss in dwarf galaxies, but for this (admittedly small) data set this appears to be a contrived solution as, from current models, this would have to preferential mass loss of massive star ($> 20M_{\odot}$) SNII products.

The observations we have presented here also add to the evidence which suggests that the abundance patterns observed in stars in small nearby galaxies are markedly different to those observed in our Galaxy. This makes it difficult for a significant proportion of the stars observed in our Galaxy to have been formed in small galaxies which subsequently merged to form the Milky Way. This is true of the disk, the bulge and inner-halo of our

Galaxy from the (limited) data available to date. The only component of our Galaxy with some similarity to the stellar populations found in dwarf galaxies is the outer-halo, which contains a very small fraction by mass of stars in our Galaxy.

With our accurate measurements of a range of different elements we have found that we can plot the enrichment of the ISM in these galaxies due to the observed star formation rate variations directly. This is especially evident in the alpha elements (see Figure 16). This is the first time such a direct *measurement* has been made of the chemical evolution of a galaxy over nearly a Hubble time. Currently the number of stars observed in each dSph is too small to be able to make concrete statements, but it is clear that larger samples coming from instruments like FLAMES, are going to have a dramatic impact upon our understanding of the chemical evolution of galaxies. These larger samples will also allow us to be more definite in our interpretation of the nucleosynthetic origin of the elements used to trace SNII and SNIa masses and rates, as well as the timescales and effect of AGB stars.

There are many good arguments to suggest that star formation has occurred in these small objects back to the earliest times in the Universe. There are also suggestions that the first stars were formed in dwarf galaxy sized objects. Nonetheless we can find no evidence that any of the stars we observed were formed from an ISM enriched by the single zero metallicity stars proposed in the literature.

The absolute ages of the oldest stars can still not be determined very accurately, a reasonable error of ~ 2 Gyr is the time elapsed between $z=6$ and $z=2$. But with abundances we can measure the enrichment of the gas in a galaxy which provides enough information to allow us to determine a more accurate absolute time scale. The galaxy must produce SN at a rate consistent with the star formation history. We have taken this approach here for a limited sample of stars with promising results, we look forward to significantly extending our sample in the not too distant future.

Acknowledgments: We thank the Paranal Observatory staff for the excellent support we received during both of our visitor runs. We also acknowledge useful discussions with Tom Abel, Andrea Ferrara, Alex Heger, Sally Oey, Evan Skillman, Rosie Wyse and Sukyoung Yi. We also thank the anonymous referee for helpful comments. ET gratefully acknowledges support from a fellowship of the Royal Netherlands Academy of Arts and Sciences, and PATT travel support from the University of Oxford. KAV would like to thank the NSF for support through a CAREER award, AST-9984073.

REFERENCES

- Aaronson M. & Mould J.R. 1980, ApJ, 240, 804
- Aaronson M. & Mould J.R. 1985, ApJ, 290, 191
- Aaronson M., Olszewski E.W. & Hodge P.W. 1983, ApJ, 267, 271
- Aaronson M., Da Costa G.S., Hartigan P., Mould J.R., Norris J. & Stockman H.S. 1984, ApJ, 277, 9
- Abel T., Bryan G.L. & Norman M.L. 2002, Science, 295, 93
- Andrews S.M., Meyer D.M. & Lauroesch J.T. 2001, ApJ, 552, L73
- Armandroff T.E. & Da Costa G.S. 1991, AJ, 101, 1329
- Azzopardi M., Lequeux J. & Westerlund B.E. 1985, A&A, 144, 388
- Azzopardi M., Lequeux J. & Westerlund B.E. 1986, A&A, 161, 232
- Azzopardi M., Breysacher J., Muratorio G. & Westerlund B.E. 1999, in IAU Symposium 192 “The Stellar Content of Local Group Galaxies”, eds. Whitelock & Cannon, p. 9
- Baade W. 1963, *Evolution of Stars and Galaxies*, ed. C. H. P. Payne-Gaposchkin (Cambridge: MIT Press)
- Beauchamp D., Hardy E., Suntzeff N.B., Zinn R. 1995, AJ, 109, 1628
- Bergbusch, P.A. & vandenBerg, D.A. 2001 ApJ, 556, 322
- Bertelli G., Bressan A., Chiosi C., Fagotto F., Nasi E. 1994 A&AS, 106, 275
- Brocato, E., Buonanno, R., Castellani, V. & Walker, A. R. 1989 ApJS, 71, 25
- Brocato, E., Castellani, V., Ferraro, F.R., Piersimoni, A.M. & Testa, V. 1996 MNRAS, 282, 614
- Bromm, V., Coppi, P.S. & Larson, R.B. 2002 ApJ, 564, 23
- Buonanno R., Corsi C. E., Fusi Pecci F., Hardy E. & Zinn R. 1985, A&A, 152, 65
- Buonanno R., Corsi C.E., Castellani M., Marconi G., Fusi Pecci F. & Zinn R. 1999, AJ, 118, 1671
- Busso *et al.* 1995 ApJ, 446, 775
- Carignan C., Beaulieu S., Côté S., Demers S. & Mateo M. 1998, AJ, 116, 1690
- Castilho, B.V., Pasquini, L., Allen, D.M., Barbuy, B. & Molaro, P. 2000 A&A, 361, 92
- Da Costa G.S. 1984 ApJ, 285, 483

- Da Costa G. S. 1994, ESO/OHP Workshop on Dwarf Galaxies, eds. G. Meylan & P. Prugniel (Garching: ESO), p.221
- Da Costa G.S. & Armandroff T.E. 1990 AJ, 100, 162
- Dekel A. & Silk J. 1986 ApJ, 303, 39
- Dekker, H., D’Odorico, S., Kaufer, A., *et al.* 2000, in “Optical and IR Telescopes Instrumentation and Detectors”, Masanori Iye and A.M Moorwood Eds., Proc. SPIE Vol. 4008, pp.534-545
- Dolphin A. 2002 MNRAS, 332, 91
- Edvardsson B., Andersen J., Gustafsson B., Lambert D. L., Nissen P. E. & Tomkin J. 1993, A&A, 275, 101. [E93]
- Ferrara A. & Tolstoy E. 2000, MNRAS, 313, 291
- Ferrara, A., Pettini, M. & Shchekinov, Y. 2000, MNRAS, 319, 539
- Ferraro F.R. et al. 1995, MNRAS, 272, 391
- Freeman K. & Bland-Hawthorn J. 2002 ARAA, in press
- Frogel J.A., Blanco V.M., Cohen J.G. & McCarthy M.F. 1982, ApJ, 252, 133
- Gallart C, Freedman W.L., Aparicio A., Bertelli G. & Chiosi C. 1999 AJ, 118, 2245
- Gilmore G. & Wyse R.F.G. 1991 ApJL, 367, 55
- Gilmore G. & Wyse R.F.G. 1998 AJ, 116, 748
- Gratton R.G. & Sneden C. 1988 A&A, 204, 193
- Heger A. & Woosley S.E. 2002 ApJ, 567, 532
- Held, E.V., Saviane, I., Momany, Y. & Carraro, G. 2000 ApJL, 530, 85
- Held, E.V., Clementini G., Rizzi, L., Momany, Y., Saviane, I. & Di Fabrizio, L. 2001 ApJL, 562, 39
- Hernandez X., Gilmore G. & Valls-Gabaud D. 2000 MNRAS, 317, 831
- Hill, V., Andrievsky, S., Spite, M. & Spite, F. 1995 A&A, 293, 347
- Hill V. 1997 A&A, 324, 435
- Hill V., Francois P., Spite M., Primas F. & Spite F. 2000 A&A, 364, L19 [H00]
- Hill V. & Spite M. (2001) in *Cosmic Evolution*, eds, E. Vangioni-Flam, R. Ferlet & M. Lemoine, Published by New Jersey: World Scientific, p.265
- Hodge P.W. & Wright F.W. 1978, AJ, 83, 228
- Hurley-Keller D., Mateo M. & Nemeč J. 1998, AJ, 115, 1840

- Hurley-Keller D., Mateo M. & Grebel E.K. 1999, *ApJL*, 523, 25
- Kaluzny J., Kubiak M., Szymanski M., Udalski A., Krzeminski W. & Mateo M. 1995, *A&AS*, 112, 407
- Kauffmann, G., White, S.D.M. & Guiderdoni, B. 1993 *MNRAS*, 264, 201
- Kleyna, J., Wilkinson, M. I., Evans, N. W., Gilmore, G. & Frayn, C. 2002, *MNRAS*, 330, 792
- Klypin, A., Kravstov, A.V., Valenzuela, O. & Prada F. 1999, *ApJ*, 522, 82
- Lambert *et al.* 1995 *ApJ*, 450, 302
- Larson R.B. 1974 *MNRAS*, 169, 229
- Mac Low, M-M. & Ferrara, A. 1999 *ApJ*, 513, 142
- Madau P., Pozzetti L. & Dickinson M. 1998, *ApJ*, 498, 106
- Madau P., Ferrara A. & Rees M.J. 2001 *ApJ*, 555, 92
- Majewski S.R., Siegel M.H., Patterson R.J. & Rood R.T. 1999, *ApJL*, 520, 33
- Mateo, M. 1998 *ARAA*, 36, 435
- Mateo, M., Hodge, P. & Schommer, R.A. 1986 *ApJ*, 311, 113
- Mateo, M., Olszewski E. W., Vogt S. S. & Keane M. J. 1998, *AJ*, 116, 2315
- Mateo, M., Olszewski E. W., Pryor C., Welch D. L. & Fischer P. 1993, *AJ*, 105, 510
- Mateo, M., Olszewski E. W., Welch D. L., Fischer P. & Kunkel W. 1991, *AJ*, 102, 914
- Mathews, G.J. & Cowan, J.J. 1990 *Nature*, 345, 491
- Mathews, G.J., Bazan, G. & Cowan, J.J. 1992 *ApJ*, 391, 719
- Matteucci F. & Tosi M. 1985, *MNRAS*, 217, 391
- Matteucci, F., Raiteri, C.M., Busson, M., Gallino, R. & Gratton, R. 1993 *A&A*, 272, 421
- McWilliam, A., Preston, G.W., Sneden, C. & Searle, L. 1995 *AJ*, 109, 2757
- McWilliam, A. & Rich, R.M 1994 *ApJS*, 91, 749
- McWilliam A. 1997 *ARAA*, 35, 503
- Mighell K. J. 1990, *A&AS*, 82, 1
- Mighell K. J. 1997, *AJ*, 114, 1458
- Monkiewicz J., Mould J.R., Gallagher J.S. & the WFPC2 IDT 1999, *PASP*, 111, 1392
- Moore B., Ghigna S., Governato F., Lake G., Quinn T., Stadel J. & Tozzi P. 1999, *ApJL*, 524, 19

- Morrison H.L. 1993, AJ, 106, 578
- Mori, M., Ferrara, A. & Madau, P. 2002 ApJ, 571, 40
- Mould J., & Aaronson M. 1983, ApJ, 273, 530
- Munari U. & Zwitter T. 1997 A&A, 318, 269
- Navarro, J.F., Frenk, C.S. & White, S.D.M. 1995 MNRAS, 275, 56
- Nissen, P.E. & Schuster, W.J. 1997 A&A, 326, 751
- Oh, K.S., Lin, D.N.C. & Aarseth, S.J. 1995 ApJ, 442, 142
- Oh, S.P., Nollett, K.M., Madau P. & Wasserburg, G.J. 2001 ApJL, 562, 1
- Pagel B.E.J. 1997 *Nucleosynthesis and the Chemical Evolution of Galaxies*, CUP, pp 236
- Pagel B.E.J. & Tautvaišienė G. 1998, MNRAS, 299, 535
- Pettini M., Ellison S.L., Steidel C.C., Shapley A.E. & Bowen D.V. 2000, ApJ, 532, 65
- Pilachowski C.A., Sneden C. & Kraft, R. P. 1996, AJ, 111, 1689
- Prantzos, N. & Silk, J. 1998 ApJ, 507, 229
- Primas F., Brugamyer E., Sneden C., King J.R., Beers T.C., Boesgaard A.M., Deliyannis C.P., 2000, in *The First Stars*, A.Weiss, T.Abel, V.Hill Editors, Springer, p.51
- Queloz D., Dubath P. & Pasquini L. 1995, A&A, 300, 31
- Rocha-Pinto, H.J., Scalo, J., Maciel, W.J. & Flynn, C. 2001, ApJL, 531, 115
- Rutledge G.A., Hesser J.E. & Stetson P.B. 1997 PASP, 109, 907
- Saha A., Seitzer P., & Monet D.G. 1986, AJ, 92, 302
- Sandage A. 1993, AJ, 106, 687
- Schweitzer A. E., Cudworth K. M., Majewski S. R. & Suntzeff N. B. 1995, AJ, 110, 2747
- Searle L. & Sargent W.L.W. 1972, ApJ, 173, 25
- Shetrone M.D. 1996, AJ, 112, 1517
- Shetrone M.D. 1998, ASP Conf. Ser. *Galactic Halos*, ed. D. Zaritsky, p.11
- Shetrone M.D., Bolte M. & Stetson P.B. 1998, AJ, 115, 1888
- Shetrone M.D., Côté P. & Stetson P.B. 2001, PASP, 113, 1122
- Shetrone M.D., Côté P. & Sargent W.L.W. 2001, ApJ, 548, 592 [SCS01]
- Shetrone M.D. *et al.* 2002, AJ, submitted [Paper I]
- Silk, J., Wyse, R.F.G. & Shields, G.A. 1987 ApJ, 322, 59

- Smecker-Hane T.A., Stetson P.B., Hesser J.E. & Lehnert M.D. 1994, *AJ*, 108, 507
- Snedden, C., Gratton, R.G., Crocker, D.A., 1991 *A&A*, 246, 354
- Steinmetz, M. & Navarro J.F. 2002 *New Astronomy*, 7, 155
- Stetson P.B., Hesser J.E. & Smecker-Hane T.A. 1998, *PASP*, 110, 533
- Tegmark, M., Silk, J., Rees, M.J., Blanchard, A., Abel, T. & Palla, F. 1997 *ApJ*, 474, 1
- Thévenin, F., Charbonnel, C., de Freitas Pacheco, J. A., Idiart, T. P., Jasniewicz, G., de Laverny, P. & Plez, B. 2001 *A&A*, 373, 905
- Timmes, F.X., Woosley, S.E. & Weaver, T.A. 1995 *ApJS*, 98, 617
- Tinsley B.M. 1979 *ApJ*, 229, 1046
- Tolstoy, E., Irwin, M.J., Cole, A.A., Pasquini, L., Gilmozzi, R. & Gallagher, J.S. 2001 *MNRAS*, 327, 918 [T01]
- Tolstoy, E. 2002, contribution to *New Horizons in Globular Cluster Astronomy*, eds. Piotto *et al.* astro/ph-0209222
- Umeda, H. & Nomoto, K. 2002 *ApJ*, 565, 385
- Unavane M., Wyse R.F.G. & Gilmore G. 1996 *MNRAS*, 278, 727
- van den Bergh S. 2000, *PASP*, 112, 529
- Venn K.A., Lennon D.J., Kaufer A., McCarthy J.K., Przybilla N., Kudritski R.P., Lemke M., Skillman E.D. & Smartt S.J. 2001, *ApJ*, 547, 765
- White, S. D. M., & Rees, M. 1978, *MNRAS*, 183, 341
- Will J.-M., Bomans D.J., Tucholke H.-J., De Boer K.S., Grebel E.K., Richtler T., Seggewiss W. & Vallenari A. 1995 *A&AS*, 112, 367
- Woosley, S. E. & Weaver, T. A. 1995, *ApJS*, 101, 181
- Young L.M. 1999, *AJ* 117, 1758
- Yi S., Demarque P., Kim Y.-C., Lee Y.-W., Ree C.-H., Lejeune Th., & Barnes S. 2001, *ApJS*, 136, 417
- Zinn R. 1980, in *Globular Clusters*, eds. D. Hanes & B. Madore (Cambridge: Cambridge Univ. Press), p. 191
- Zinn R. 1993, in ASP Conf. Ser. *The Globular Cluster-Galaxy Connection*, eds Smith & Brodie, p.302

Table 1: The Dwarf Spheroidal Galaxies

Object	l	b	(m-M) ₀ mag	E(B-V) mag	M _V mag	Σ ₀ mag/arcsec ²	v _r km/s	M _{tot} 10 ⁶ M _⊙
Sculptor	287.5	−83.2	19.54±0.08	0.02±0.02	−11.1	23.7±0.4	110±3	6.4
Carina	260.1	−22.2	20.03±0.09	0.025±0.02	−9.3	25.5±0.4	224±3	13
Leo I	226.0	+49.1	21.99±0.20	0.01±0.01	−11.9	22.4±0.3	286±2	22
Fornax	237.1	−65.7	20.70±0.12	0.03±0.01	−13.2	23.4±0.3	53±3	68
Draco	86.4	+34.7	19.58±0.15	0.03±0.01	−8.8	25.3±0.5	−293±2	22
Ursa Minor	105.0	+44.8	19.11±0.10	0.03±0.02	−8.9	25.5±0.5	−248±2	23
Sextans	243.5	+42.3	19.67±0.08	0.03±0.01	−9.5	26.2±0.5	227±3	19

all these data are taken from Mateo 1998

Table 2: Isochrone Ages & α -Abundances in UVES Dwarf Spheroidal stars

Galaxy	star id	age (Gyr)	[FeI/H]	[O/Fe]	[Mg/Fe]	[Ca/Fe]	[α /Fe]
Sculptor	H459	15_{-3}^{+1}	-1.66 ± 0.02	0.12 ± 0.15	0.36 ± 0.13	0.24 ± 0.05	0.18
	H479	15_{-0}^{+1}	-1.77 ± 0.02	0.38 ± 0.11	0.26 ± 0.16	0.17 ± 0.05	0.13
	H461	15_{-0}^{+1}	-1.56 ± 0.02	0.34 ± 0.16	0.18 ± 0.11	0.22 ± 0.06	0.13
	H482	10_{-2}^{+5}	-1.24 ± 0.02	0.08 ± 0.18	0.09 ± 0.13	0.06 ± 0.06	-0.01
	H400	15_{-0}^{+1}	-1.98 ± 0.03	–	0.37 ± 0.12	0.38 ± 0.09	0.23
Fornax	M12	15_{-3}^{+1}	-1.60 ± 0.02	0.12 ± 0.18	0.09 ± 0.07	0.23 ± 0.06	0.12
	M25	10_{-3}^{+5}	-1.21 ± 0.02	0.07 ± 0.11	0.02 ± 0.09	0.21 ± 0.06	0.03
	M21	$2_{-1}^{+0.1}$	-0.67 ± 0.03	0.02 ± 0.17	0.20 ± 0.12	0.23 ± 0.08	0.27
Leo I	M5	8_{-3}^{+3}	-1.52 ± 0.02	0.43 ± 0.13	0.12 ± 0.12	0.15 ± 0.06	0.13
	M2	$2_{-1}^{+0.5}$	-1.06 ± 0.02	-0.04 ± 0.13	-0.19 ± 0.19	0.02 ± 0.06	-0.08
Carina	M4	11_{-3}^{+4}	-1.59 ± 0.02	0.12 ± 0.09	0.26 ± 0.09	0.14 ± 0.04	0.14
	M3	13_{-3}^{+3}	-1.65 ± 0.02	-0.06 ± 0.12	-0.27 ± 0.12	-0.10 ± 0.06	-0.26
	M2	10_{-2}^{+2}	-1.60 ± 0.02	0.34 ± 0.12	0.23 ± 0.10	0.20 ± 0.05	0.17
	M12	5_{-1}^{+2}	-1.41 ± 0.02	0.07 ± 0.10	0.24 ± 0.10	0.12 ± 0.05	0.13
	M10	15_{-0}^{+1}	-1.94 ± 0.02	-0.02 ± 0.19	0.06 ± 0.11	-0.02 ± 0.05	0.05

Table 3: Isochrone Ages for Dwarf Spheroidal stars measured by SCS01

Galaxy	star id	age (Gyr)	[FeI/H]	[α /Fe]
Draco	11	9	-1.72 ± 0.11	0.11 ± 0.05
	343	10	-1.86 ± 0.11	0.01 ± 0.07
	473	6	-1.44 ± 0.07	0.09 ± 0.07
	267	15	-1.67 ± 0.13	0.15 ± 0.07
	24	15	-2.36 ± 0.09	0.08 ± 0.05
	119	15	-2.97 ± 0.15	0.11 ± 0.06
Ursa Minor	177	15	-2.01 ± 0.11	0.19 ± 0.05
	297	15	-1.68 ± 0.11	0.10 ± 0.05
	K(C2)	15	-2.17 ± 0.12	0.25 ± 0.07
	O	15	-1.91 ± 0.11	0.17 ± 0.05
	199	15	-1.40 ± 0.11	-0.03 ± 0.06
Sextans	168	15	-2.18 ± 0.12	0.10 ± 0.10
	35	15	-1.93 ± 0.11	0.13 ± 0.06
	DC5	15	-1.93 ± 0.11	0.12 ± 0.07
	49	15	-2.85 ± 0.13	-0.01 ± 0.11
	58	6	-1.45 ± 0.12	-0.26 ± 0.07
	36	15	-2.19 ± 0.12	0.10 ± 0.07

Table 4: Heavy Element and Iron-Peak Abundances in UVES Dwarf Spheroidal stars

Galaxy	star id	[Ba/Eu]	[Mn/Fe]	[Zn/Fe]	[Cu/ α]
Sculptor	H459	−0.30	−0.52	0.27	−1.23
	H479	−0.44	−0.52	−0.38	−0.96
	H461	−0.14	−0.62	−0.33	−0.92
	H482	0.03	−0.39	0.08	−1.12
	H400	−0.27	–	–	< −0.69
Fornax	M12	−0.31	−0.47	−0.29	−0.79
	M25	0.23	−0.43	0.00	−0.63
	M21	0.32	−0.61	–	0.12
Leo I	M5	−0.39	−0.48	−0.31	−0.73
	M2	−0.25	−0.31	−1.46	−0.47
Carina	M4	−0.17	−0.46	−0.10	−0.77
	M3	−0.19	−0.18	−0.30	−0.59
	M2	0.04	−0.50	0.04	−0.80
	M12	0.07	−0.45	−0.22	−0.74
	M10	−0.55	−0.47	−0.20	< −0.65

Table 5: Metallicity Spreads: photometric versus spectroscopic

Galaxy	Photometric $\langle [Fe/H] \rangle$	$\delta[Fe/H]$	Spectroscopic $\langle [Fe/H] \rangle$	$\delta[Fe/H]$	
Ursa Minor	-2.2	0.1	-1.9	1.4	SCS01
Draco	-2.1	0.2	-2.0	1.5	SCS01
Carina	-2.0	0.2	-1.6	0.5	this work
Sculptor	-1.8	0.1	-1.5	0.9	this work
Sextans	-1.7	0.2	-2.1	0.7	SCS01
Leo I	-1.5	0.4	-1.3:	0.5:	this work
Fornax	-1.3	0.2	-1.2	1.0	this work

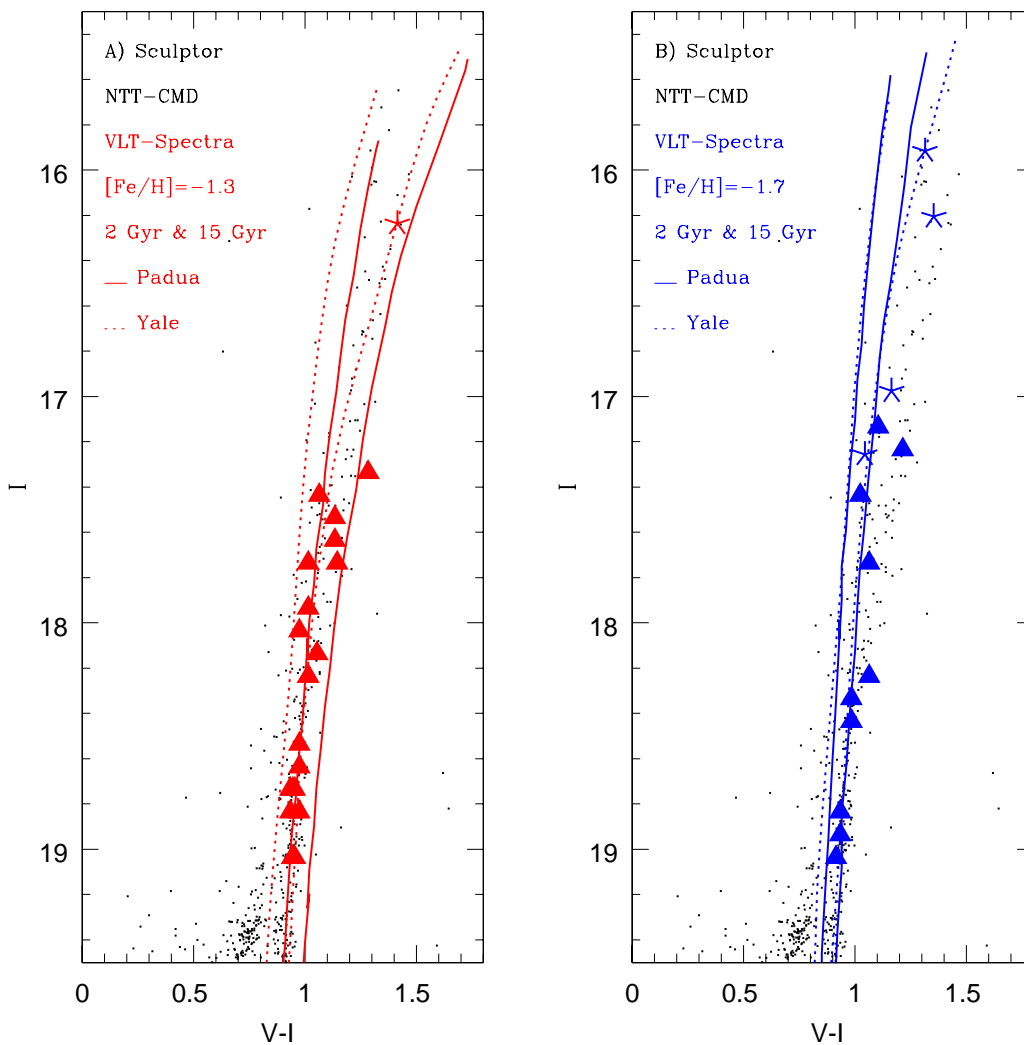


Fig. 1.— The positions of our UVES targets (*stars*) and the CaT targets from T01 (*filled triangles*) on the RGB in Sculptor. Photometry from NTT images by Tolstoy *et al.*, in prep. Left panel shows targets with $[\text{Fe}/\text{H}] = -1.3 \pm 0.3$ and isochrones from Bertelli *et al.* (1994 = Padua) and Yi *et al.* (2001 = Yale). Similarly, the right panel shows the locations of targets with $[\text{Fe}/\text{H}] = -1.7 \pm 0.3$. This figure highlights the difficulties in determining accurate ages from isochrones even when the metallicity is known.

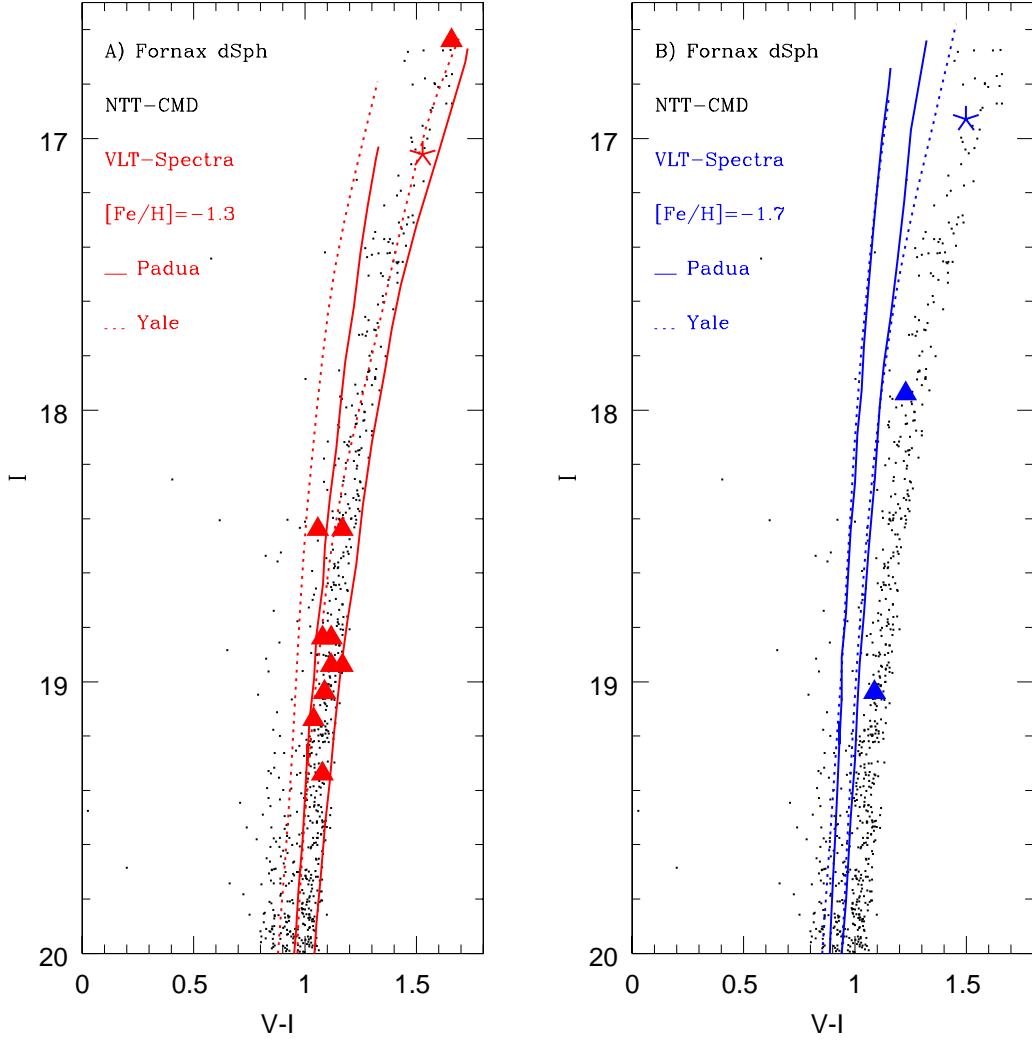


Fig. 2.— Same as Figure 1, but for imaging of and targets in Fornax.

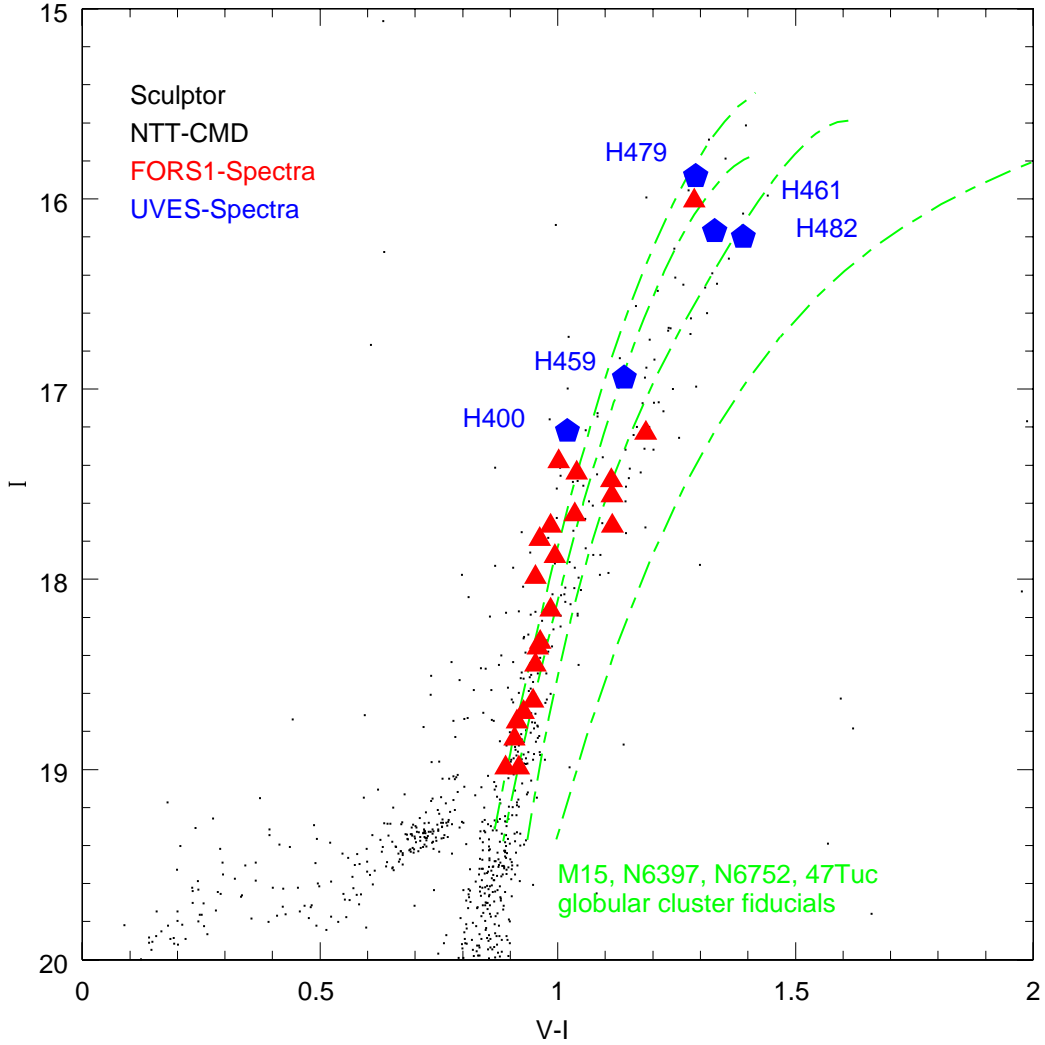


Fig. 3.— Combined CMD for Sculptor from three NTT fields. All of the CaT (*filled triangles*, from T01) and UVES (*filled pentagons*) targets are marked. *Dashed lines* are the RGB fiducials for the globular clusters: M15, NGC 6397, NGC 6752, and 47 Tucanae with metallicities $[\text{Fe}/\text{H}] = -2.2, -1.9, -1.5, -0.7$, respectively, from left to right (from Da Costa & Armandroff 1990).

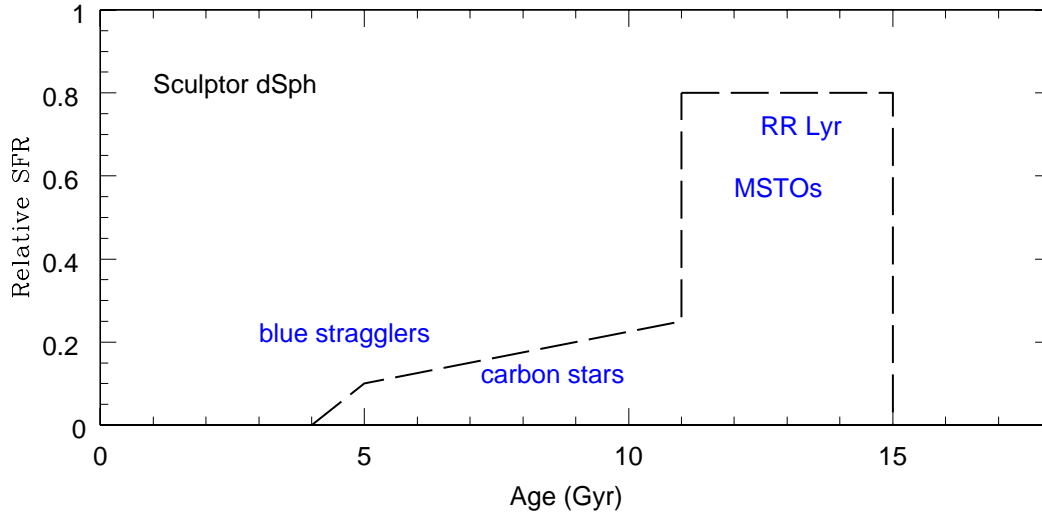


Fig. 4.— A star formation schematic for Sculptor that is consistent with its stellar population and considering how its star formation rate is likely to have varied since the epoch of globular cluster formation around 15 Gyr ago (data sets are discussed in Section 3.3.1). The stellar evolution phases used to determine the star formation rate at various ages are labelled.

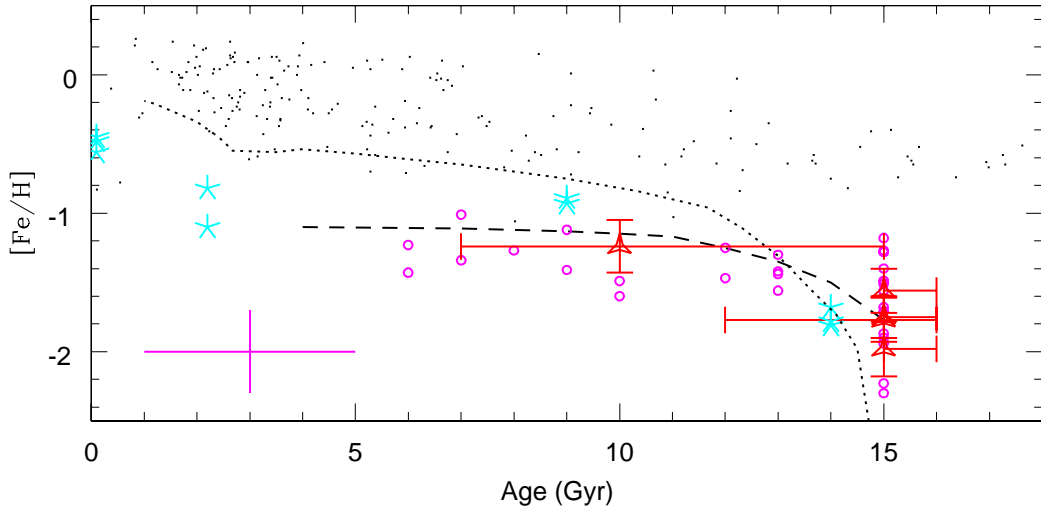


Fig. 5.— A chemical evolution scenario for Sculptor over its entire star-forming history (~ 15 Gyr). Ages have been determined by fitting theoretical isochrones to the stars RGB positions, given each stellar metallicity (discussed in Section 3.2; also see Figure 1). The dashed line adopts the SFH shown in Figure 4. The dotted line is the LMC age-metallicity relation for the bursting model by Pagel & Tautvaišienė (1998). CaT measurements of metallicity from T01 (*small circles*) assume $[\text{Ca}/\text{Fe}] = 0$; the typical error bar per CaT observation is noted in the lower left. Direct iron abundances from our UVES spectra (*filled triangles with error bars*) are in good agreement with the CaT measurements. LMC star cluster iron abundances by H00 (*stars*) are offset from the LMC bursting model, but have similar iron abundances as the Sculptor stars at the oldest ages. The numerous small dots show the iron abundances in Galactic disk stars by E93.

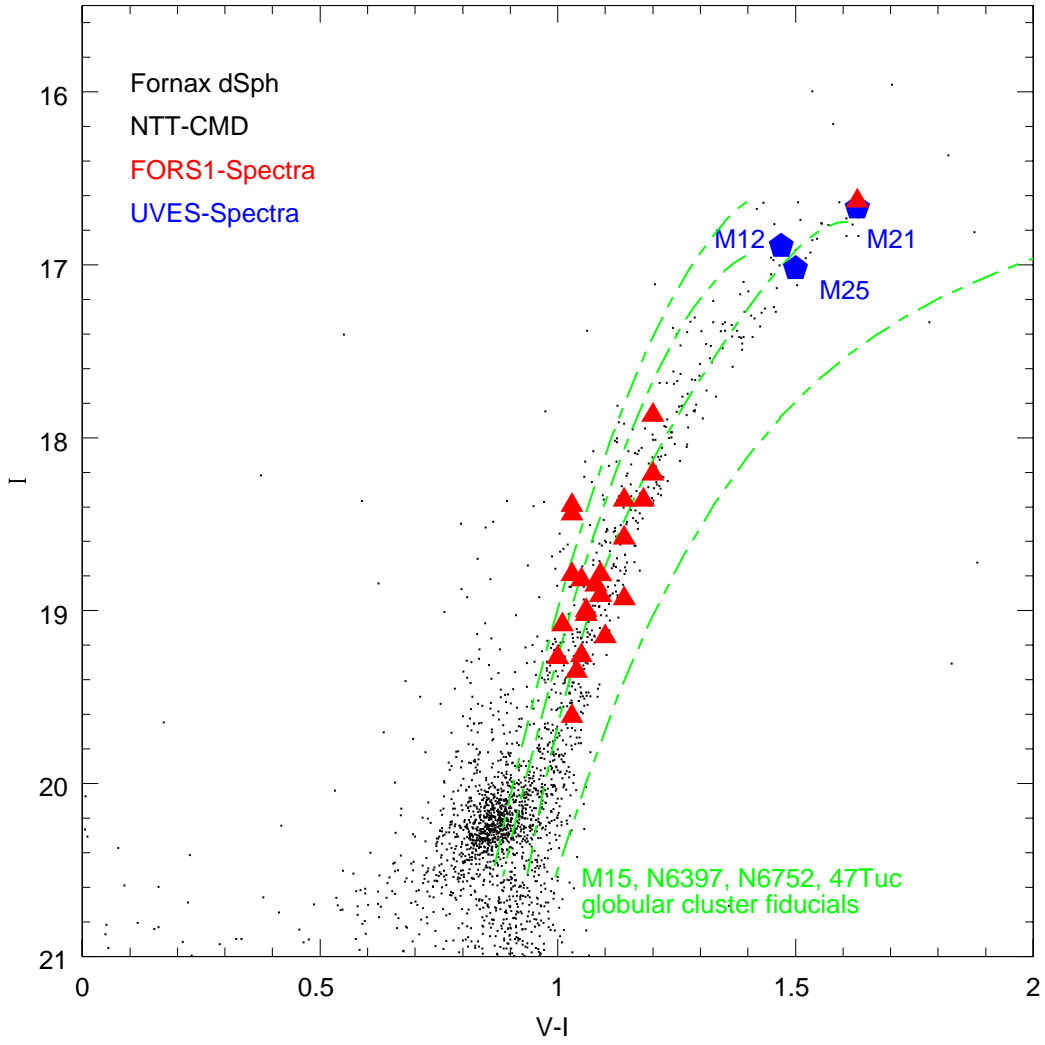


Fig. 6.— Same as Figure 3, but for targets in Fornax.

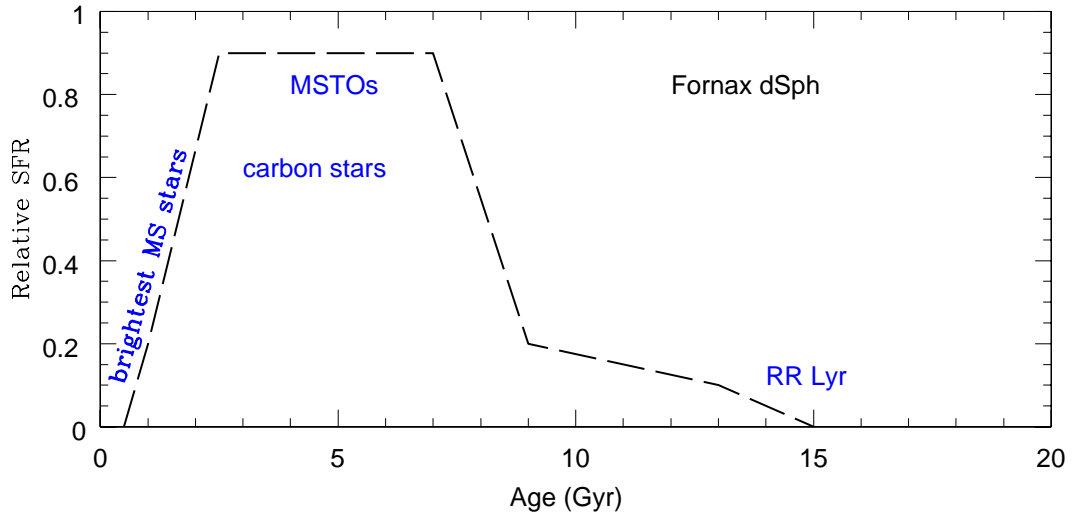


Fig. 7.— Same as Figure 4, but a schematic star formation history for Fornax (data sets are discussed in Section 3.4.1).

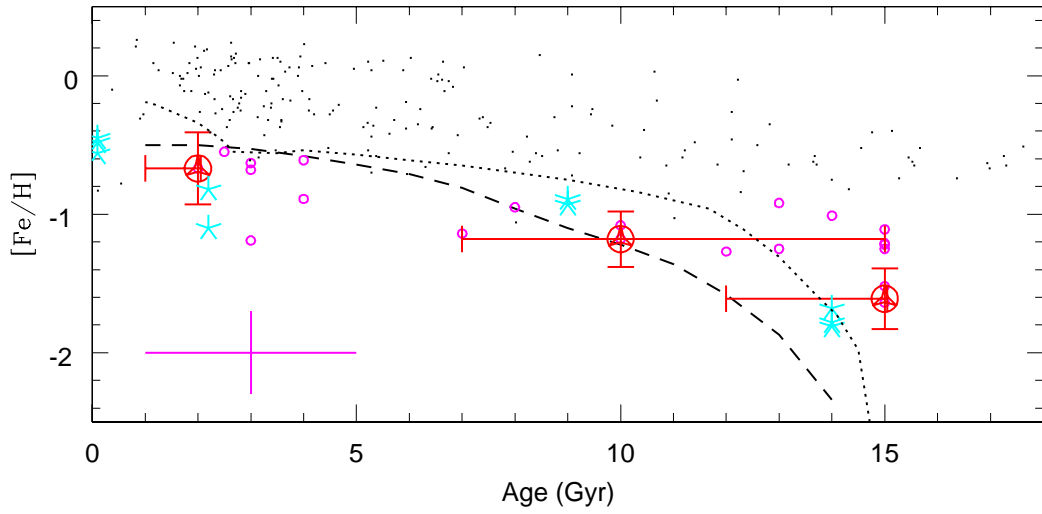


Fig. 8.— Same as Figure 6, but a chemical evolution scenario for Fornax. The dashed line adopts the SFH shown in Figure 7. The iron abundances from the UVES Fornax targets are marked by *filled triangles with circles* and error bars.

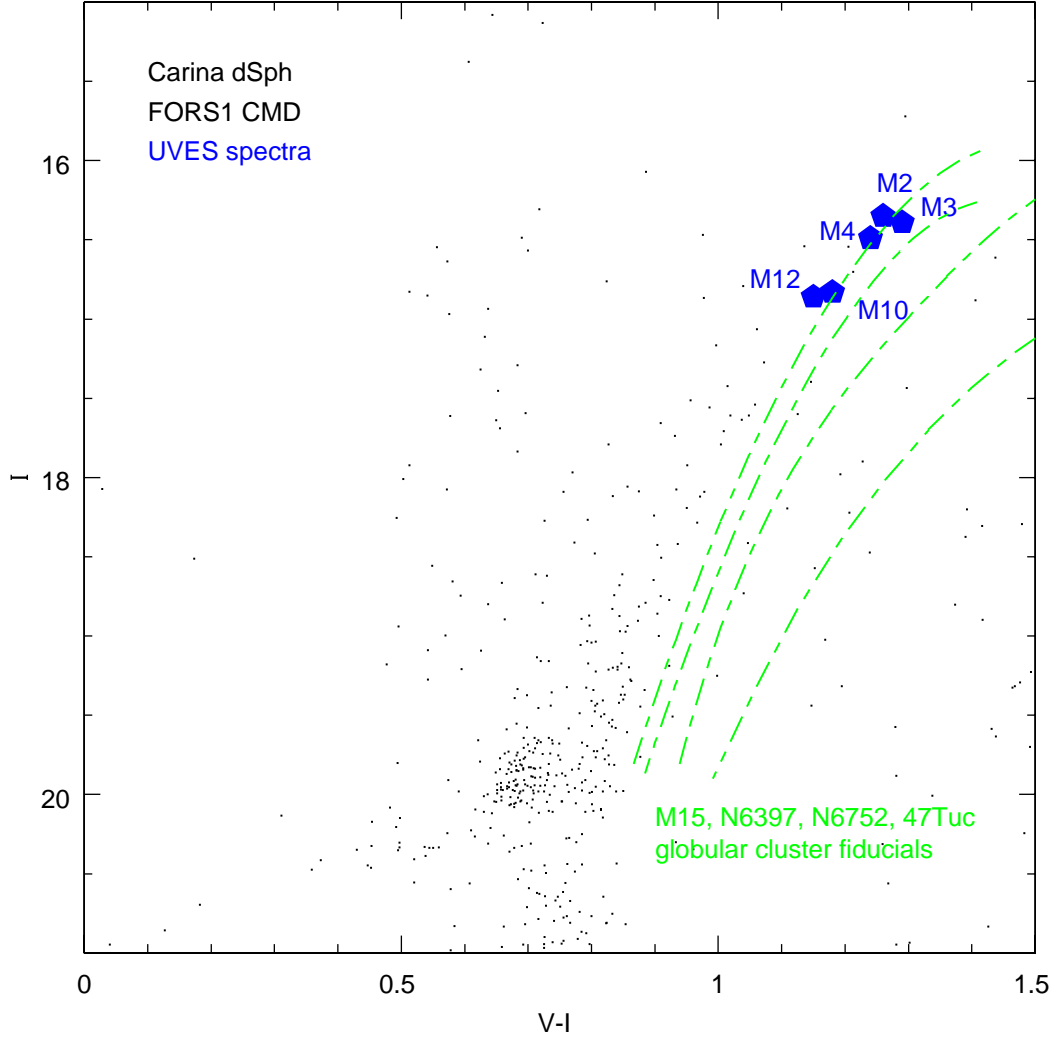


Fig. 9.— Same as Figure 3, but for targets in Carina. The CMD comes from VLT/FORS1 archival imaging data.

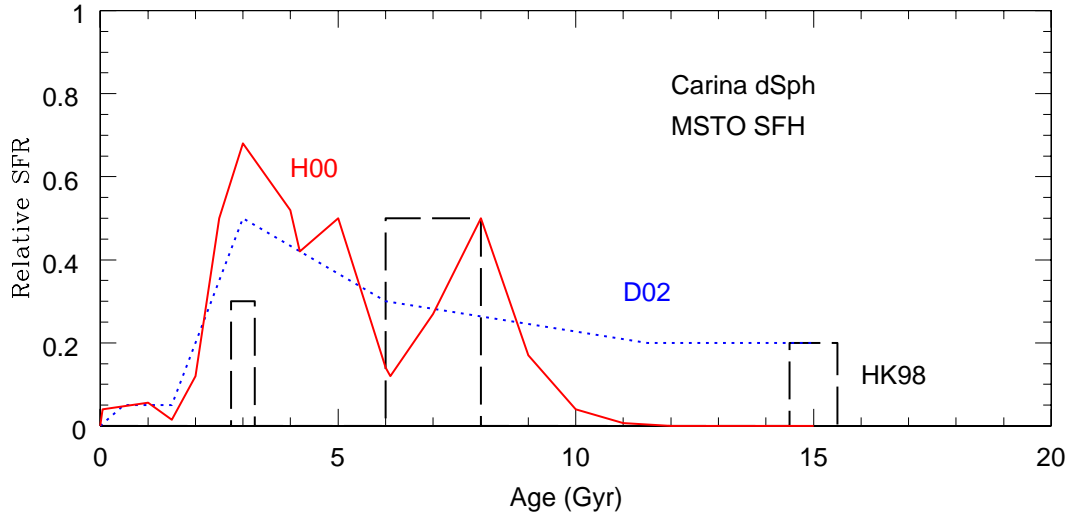


Fig. 10.— Same as Figure 4, but a schematic star formation history for Carina. Dashed lines from Hurley-Keller *et al.* (1998 = HK98) from wide-field ground-based CTIO imaging. The solid line (Hernandez *et al.* 2000 = H00) and dotted line (Dolphin 2002 = D02) are based on models that use the same HST/WFPC2 dataset. Details on these SFHs are discussed in Section 3.5.1.

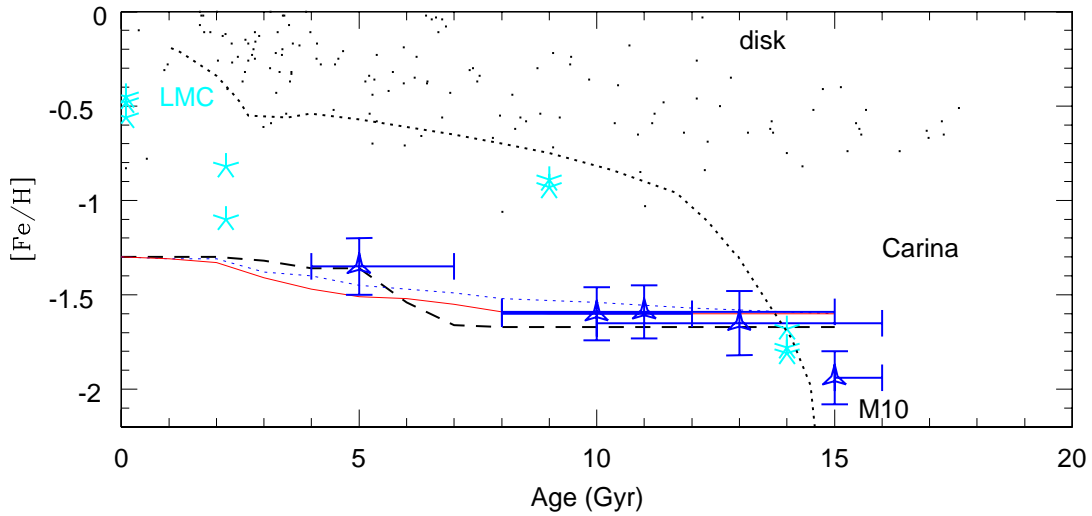


Fig. 11.— Same as Figure 5, but a chemical evolution scenario for Carina. The grouped solid, dashed, and dotted lines adopt the corresponding SFHs displayed in Figure 13. The iron abundances from the UVES Carina targets are marked by *filled triangles* with error bars.

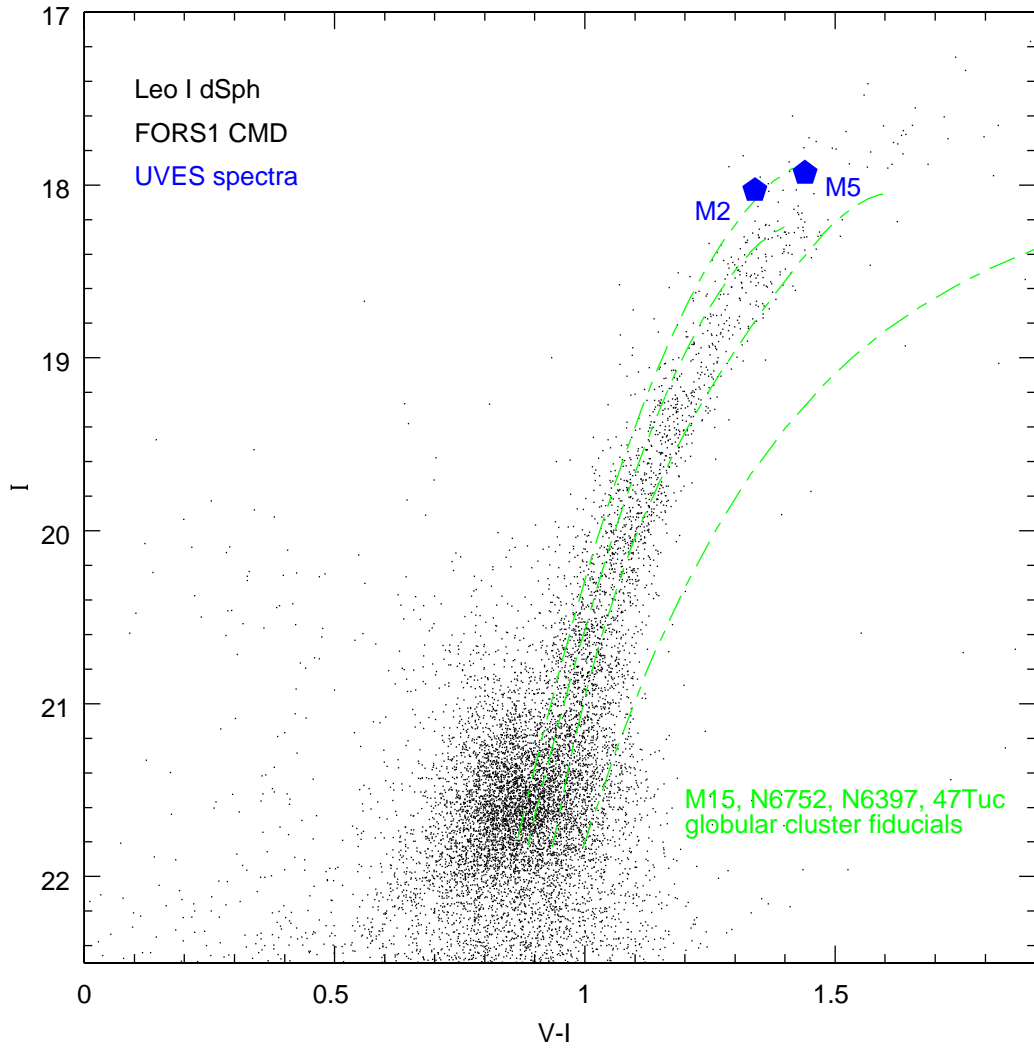


Fig. 12.— Same as Figure 9, but for targets in Leo I. The CMD comes from VLT/FORS1 archival imaging data.

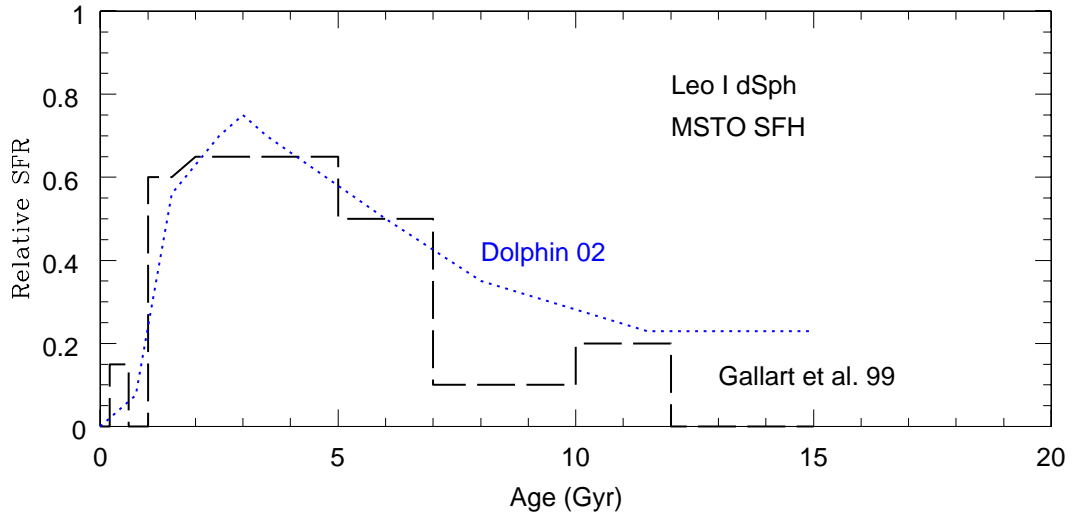


Fig. 13.— Same as Figure 4, but a schematic star formation history for Leo I Dashed line (Gallart *et al.* 1999) and dotted line (Dolphin 2002) are based on the same HST/WFPC2 data. Details on these SFHs are discussed in Section 3.6.1.

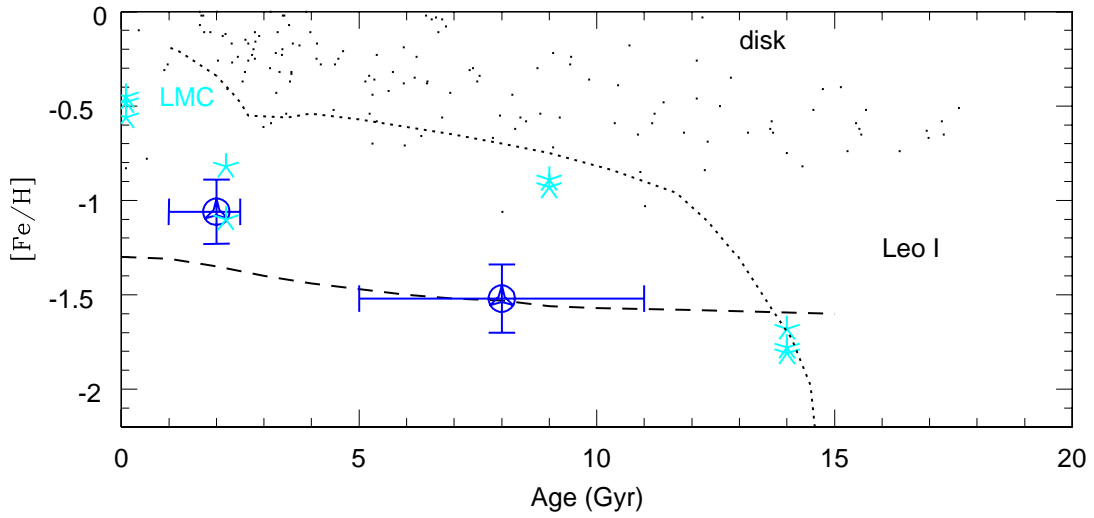


Fig. 14.— Same as Figure 6, but a chemical evolution scenario for Leo I. The SFHs in Figure 13 are so similar that they produce almost the same chemical evolution history (*dashed line*). The iron abundances from the UVES Leo I targets are marked by *filled triangles with circles* with error bars.

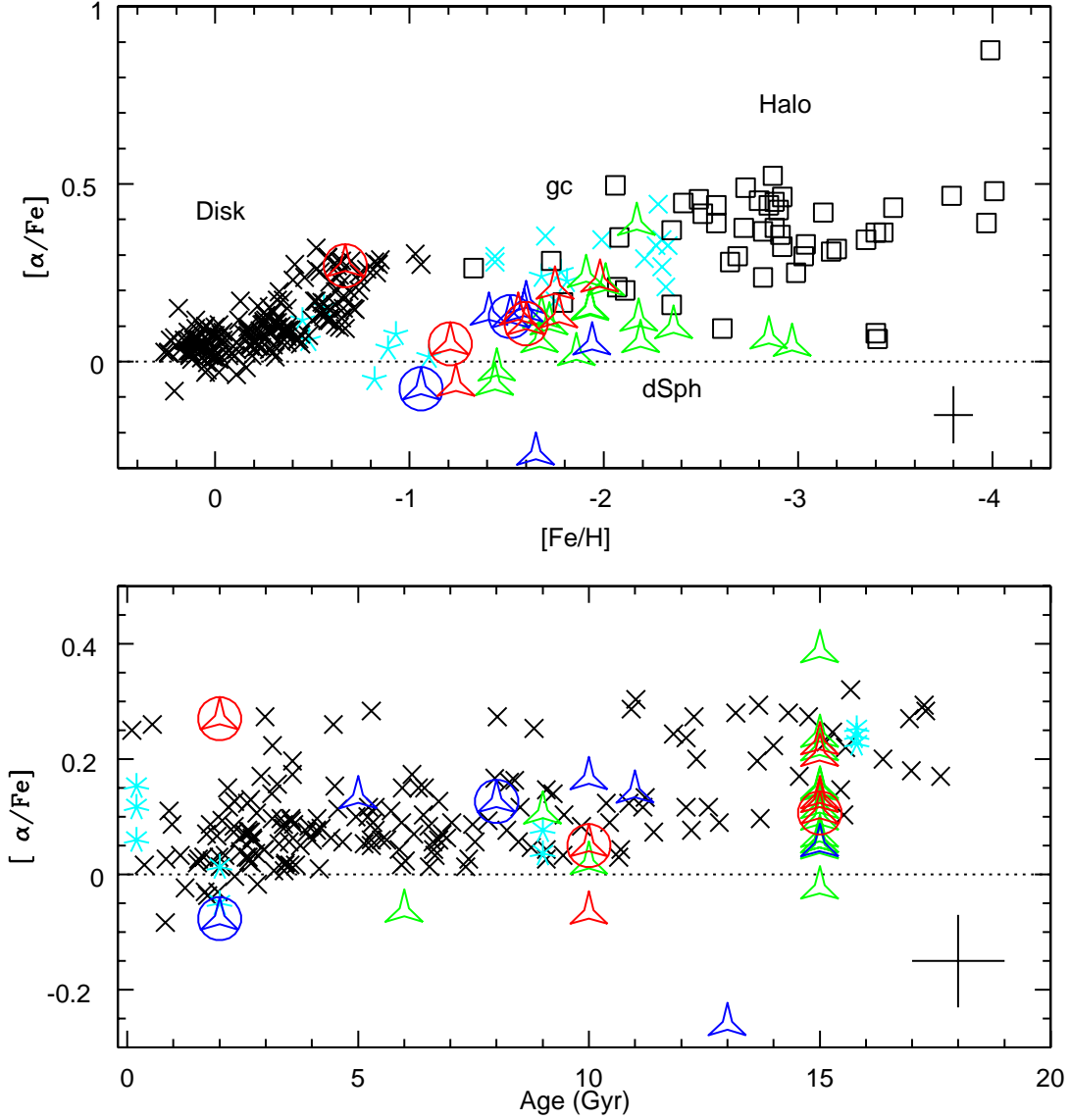


Fig. 15.— α -Element abundances, where $[\alpha/\text{Fe}] = 1/3 ([\text{Mg}/\text{Fe}] + [\text{Ca}/\text{Fe}] + [\text{Ti}/\text{Fe}])$. Our UVES α -abundances are plotted versus $[\text{Fe}/\text{H}]$ in the upper panel and versus age determined from isochrone analysis in the lower panel. The symbols are: blue triangles are the Carina data; blue triangle plus circle are Leo I data; red triangles are Sculptor data; and the red triangle plus circle are Fornax data. The green triangles are data on Draco, Ursa Minor, Sextans from SCS01. The black crosses are Galactic disk star measurements from E93; the open squares are halo data from McWilliam et al. 1995 and the light blue stars are UVES data from a study of LMC star clusters of different ages from H00. There are also light blue crosses which are our Galactic globular cluster measurements, combined with those of SCS01. We have plotted an average representative set of error bars in each plot. These plots highlight the differences between the α -element abundances observed in different environments, which are labelled in the upper plot (where gc stands for globular clusters).

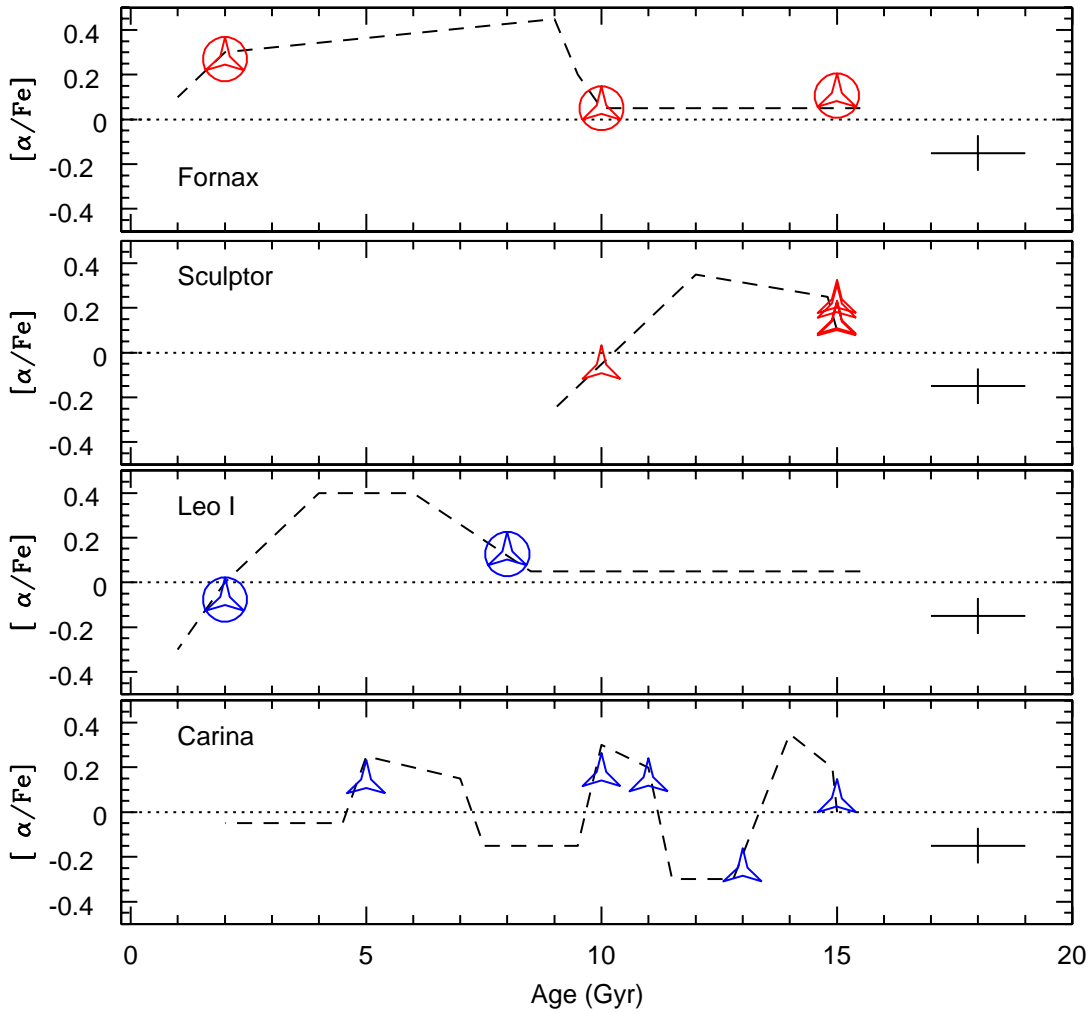


Fig. 16.— Here we plot an *illustrative* scenario which might allow us to tie in our determinations of star formation history with α -element abundances for each galaxy. The symbols are defined as in Figure 15, and representative error bars are plotted. It is obvious that the dashed lines cannot be constrained with the few data we have.

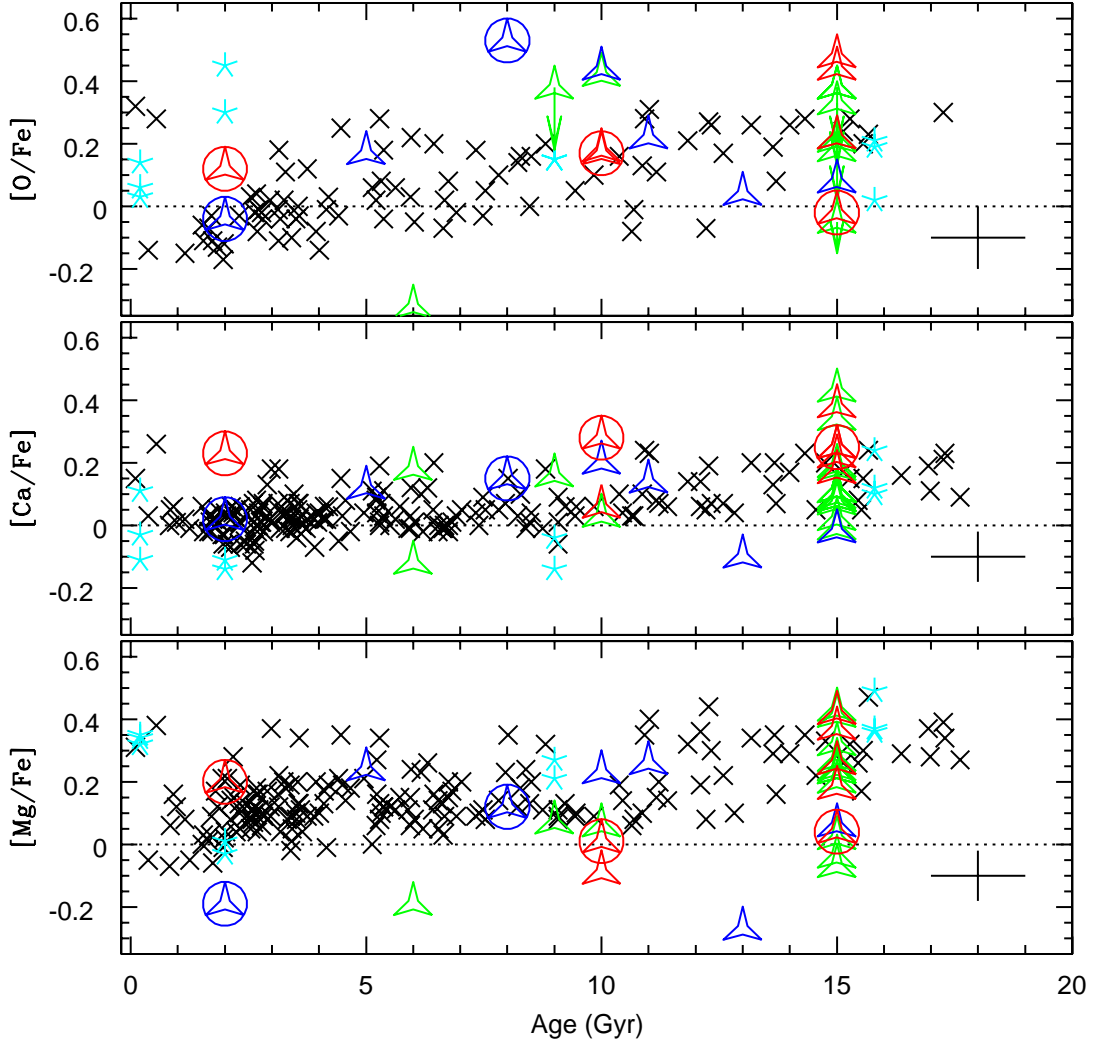


Fig. 17.— α -Element abundances: Oxygen, Calcium & Magnesium. Our UVES abundances are plotted versus age determined from isochrone analysis described in §3.2. The symbols are defined as in Figure 15.

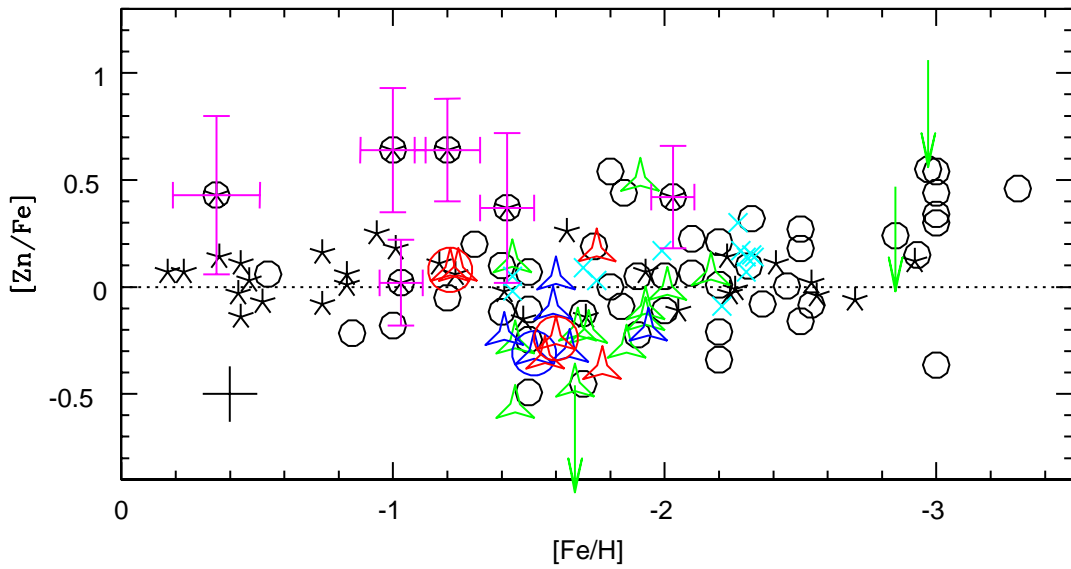


Fig. 18.— Iron-Peak Abundances: Zinc. $[Zn/Fe]$ in the dSphs (symbols as in Figure 15) compared to abundances in DLAs (*open circles* with error bars) from Pettini *et al.* (2000), and Galactic halo stars (*stars* from Sneden *et al.* 1991; *small open circles* without error bars from Primas *et al.* 2000). A representative error bar for the stellar abundances is shown in the lower left.

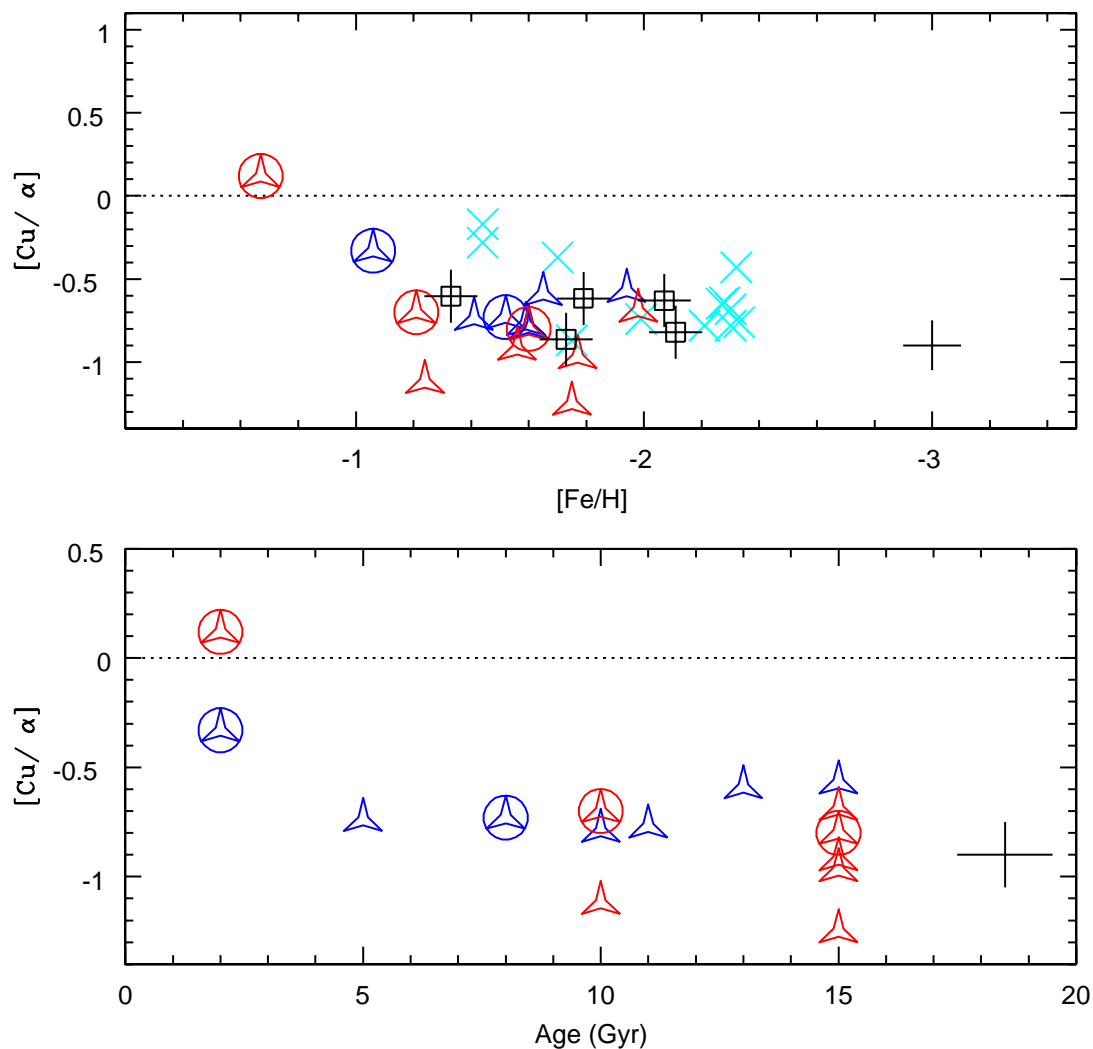


Fig. 19.— $[Cu/\alpha]$ versus $[Fe/H]$ (top panel) and age (lower panel) in our dSph stars to examine the nucleosynthetic source for Cu. Since Cu/alpha is quite flat over a wide range in metallicity and age, then we suggest that Cu is not a SN Ia product (see Paper I for further discussion). The dSph symbols are the same as in Figure 15, with the addition of *open squares* with error bars for Galactic halo stars from Gratton & Sneden (1988). The large cross symbols are our globular cluster measurements. Representative error bars are shown in the lower right of both panels.

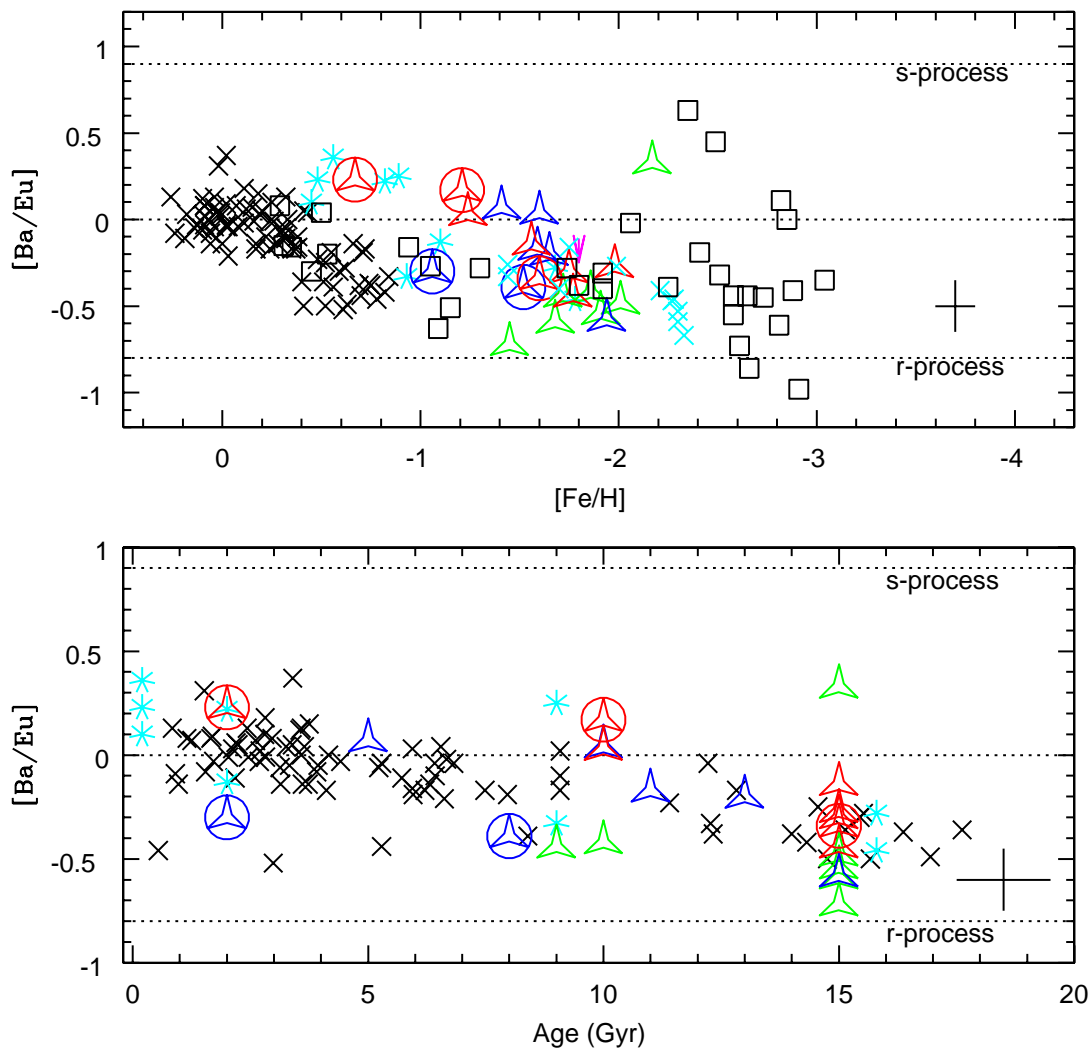


Fig. 20.— Heavy Element Abundances: Barium & Europium. $[Ba/Eu]$ versus $[Fe/H]$ (top panel) and age (lower panel) in our dSph stars to examine contributions from the s-process by AGB stars, particularly at intermediate and young ages. Symbols are the same as in Figure 15. Representative error bars are shown in the lower right of both panels.

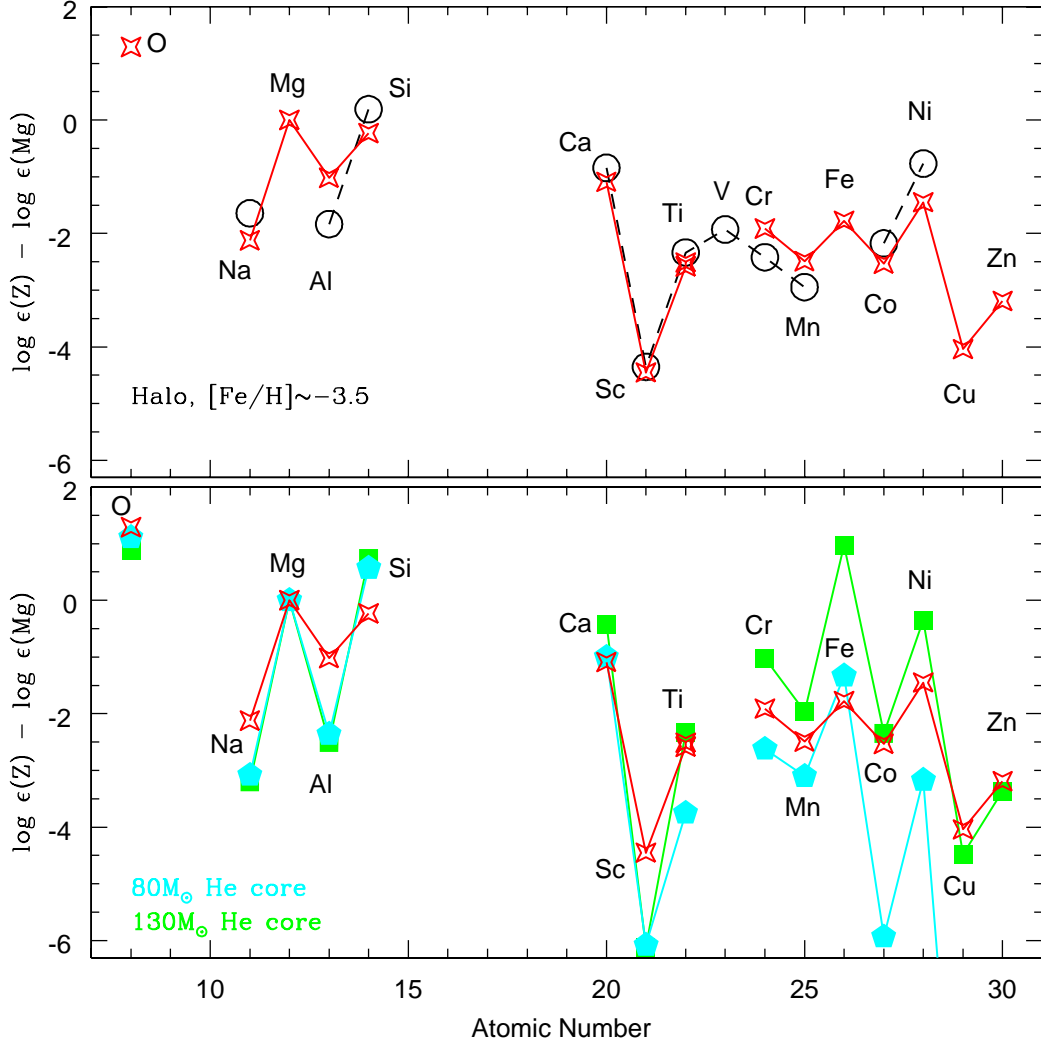


Fig. 21.— In the lower panel we show two comparisons with massive star nucleosynthesis yield predictions of Heger & Woosley (2002) and the implied yields from our abundance measurements for the oldest stars in the Sculptor dSph galaxy. In the upper panel we show in the same manner the comparison between the old stars in Sculptor and an average of the most metal poor stars observed in the Galactic halo ($-4 < [\text{Fe}/\text{H}] < -3$) taken from McWilliam et al. (1995). All the abundances plotted here are normalized to Mg.